university of groningen

University Medical Center Groningen

University of Groningen

Childhood-onset movement disorders

Lambrechts, Roald Alexander

DOI:
10.33612/diss.101316004

IMPORTANT NOTE: You are advised to consult the publisher's version (publisher's PDF) if you wish to cite from it. Please check the document version below.

Document Version
Publisher's PDF, also known as Version of record

Publication date:
2019

Link to publication in University of Groningen/UMCG research database

Citation for published version (APA):
Lambrechts, R. A. (2019). *Childhood-onset movement disorders: mechanistic and therapeutic insights from Drosophila melanogaster*. [Thesis fully internal (DIV), University of Groningen]. Rijksuniversiteit Groningen. https://doi.org/10.33612/diss.101316004

Copyright
Other than for strictly personal use, it is not permitted to download or to forward/distribute the text or part of it without the consent of the author(s) and/or copyright holder(s), unless the work is under an open content license (like Creative Commons).

The publication may also be distributed here under the terms of Article 25fa of the Dutch Copyright Act, indicated by the “Taverne” license. More information can be found on the University of Groningen website: https://www.rug.nl/library/open-access/self-archiving-pure/taverne-amendment.

Take-down policy
If you believe that this document breaches copyright please contact us providing details, and we will remove access to the work immediately and investigate your claim.

Downloaded from the University of Groningen/UMCG research database (Pure): http://www.rug.nl/research/portal. For technical reasons the number of authors shown on this cover page is limited to 10 maximum.

Download date: 23-03-2025

Chapter 4

Extracellular 4'-phosphopantetheine is a source for intracellular coenzyme A synthesis

[1]B. Srinivasan, [1]M. Baratashvili, [1]M. Van der Zwaag, [1]B. Kanon, [2]C. Colombelli, [1]R.A. Lambrechts, [1]O. Schaap, [3]E.A.A. Nollen, [4]A. Podgoršek, [4]G. Kosec, [4]H. Petković, [5]S. Hayflick, [2]V. Tiranti, [6]D.J. Reijngoud, [1]N.A. Grzeschik, [1]O. C.M. Sibon

[1] Department of Cell Biology, University Medical Center Groningen, Groningen, the Netherlands.
[2] Unit of Molecular Neurogenetics, Foundation IRCCS Neurological Institute C. Besta, Milan, Italy.
[3] European Research Institute for the Biology of Aging, University of Groningen, Groningen, the Netherlands.
[4] Acies Bio, Ljubljana, Slovenia.
[5] Departments of Molecular and Medical Genetics, Pediatrics, and Neurology, Oregon Health & Science University, Portland, Oregon, USA.
[6] Department of Laboratory Medicine, Center for Liver Digestive and Metabolic Diseases, University Medical Center Groningen, Groningen, the Netherlands.

Published in Nature Chemical Biology, 2015; 11: 784-92.

ABSTRACT

The metabolic cofactor Coenzyme A (CoA) gained renewed attention because of its role in neurodegeneration, protein acetylation, autophagy and signal transduction. The longstanding dogma is that eukaryotic cells obtain CoA exclusively via the uptake of extracellular precursors, especially vitamin B5, which is intracellularly converted through five conserved enzymatic reactions into CoA. We demonstrate that cells and organisms possess an alternative mechanism to influence intracellular CoA levels with the use of exogenous CoA. CoA is hydrolyzed extracellularly by ecto-nucleotide-pyrophosphatases to 4'-phosphopantetheine, a biologically stable molecule, able to translocate through membranes via passive diffusion. Inside the cell, 4'-phosphopantetheine is enzymatically converted back to CoA by the bifunctional enzyme CoA synthase. Phenotypes induced by intracellular CoA deprivation are reversed when exogenous CoA is provided. Our findings answer long-standing questions in fundamental cell biology and have major implications for understanding CoA-related diseases and therapies.

INTRODUCTION

Coenzyme A (CoA) was identified more than 60 years ago[1] and as a carrier of acyl groups, CoA is essential for over 100 metabolic reactions. It is estimated that CoA is an obligatory cofactor for 9% of known enzymatic reactions[2]. CoA and acetyl-CoA influence protein acetylation levels in various model organisms[3-5]. Protein acetylation is an essential posttranslational modification, catalyzed by acetyltransferases that use acetyl-CoA as the source[6]. Acetyl-CoA levels also affect autophagy[7, 8], and CoA promotes oocyte survival in *Xenopus laevis* by binding to and activating calcium/calmodulin-dependent protein kinase II (CaMKII)[9]. Taken together, intracellular concentrations of acetyl-CoA and CoA are critical to a broad range of cellular processes[10].

Current thinking about how cells and organisms obtain this indispensable molecule originates from experiments performed in the 1950's[2, 11], which demonstrate how a specific sequential order of enzymatic activities result in the formation of CoA *in vitro* when Vitamin B5 was used as a substrate. These enzymes are, in order, pantothenate kinase (PANK); phosphopantothenoylcysteine synthetase (PPCS); phosphopantothenoylcysteine decarboxylase (PPCDC); phosphopantetheine adenylyltransferase (PPAT) and dephosphoCoA kinase (DPCK) (Figure 1a). Later, genes encoding these enzymes were identified in a wide range of organisms[2, 12-14 and references therein]. In some organisms, including *Drosophila melanogaster*, mice and humans, PPAT and DPCK enzyme activities are combined into a single bifunctional protein, referred to as CoA synthase or COASY[12, 13, 15]. *In vitro* experiments show that in addition to Vitamin B5, pantetheine can also be phosphorylated by pantothenate kinase activity, and the formed product, 4'-phosphopantetheine, can serve as a precursor for CoA[16]. However, direct evidence that cells take up intact pantetheine and utilize it for CoA biosynthesis is still lacking.

In addition to renewed interest in the CoA molecule and its cellular roles, the biosynthetic route gained attention because of its connection with specific forms of neurodegeneration. Two enzymes in the CoA *de novo* biosynthetic route, PANK (first step) and COASY (combined last 2 steps) are associated with a neurodegenerative disease classified as NBIA (Neurodegeneration with Brain Iron Accumulation)[17, 18]. Mutations in the gene encoding PANK2 (one of four human PANK genes) cause an NBIA disorder, called pantothenate kinase-associated neurodegeneration (PKAN)[18]. Patients experience progressive dystonia and accumulate iron in specific brain regions. Recently, patients with mutations in the gene encoding COASY were identified and they have similar clinical features and brain iron accumulation. This new NBIA disorder is referred to as CoPAN, for COASY protein-associated neurodegeneration[17]. This strongly suggests that impairment of the classic CoA biosynthetic route underlies progressive neurodegeneration in these patient groups. Currently there is no treatment available to halt or reverse the neurodegeneration in these CoA-related disorders.

CoA levels are decreased in a *Drosophila* model for PKAN and the neurodegenerative phenotypes and decreased CoA levels are rescued by addition of pantethine to the food[19]. Pantethine addition also rescues a ketogenic diet-induced neurodegenerative phenotype in *PANK2*$^{-/-}$ knock out mice[20]. These studies demonstrate that in a pantothenate kinase impaired background, CoA precursors other than vitamin B5

can alleviate neurodegenerative symptoms. How pantethine exerts its rescuing function (especially in the mouse study) is unclear because pantethine is highly unstable in serum and rapidly converted into Vitamin B5 and cysteamine by pantetheinases[20, 21].

The aim of this study was to determine whether alternate routes exist for cells and organisms to obtain CoA. We found that extracellular CoA levels influence intracellular CoA levels both *in vitro* and *in vivo*. We showed that CoA is not a biologically stable molecule and cells do not take up CoA directly. We presented evidence that ecto-nucleotide-pyrophosphatases hydrolyzed CoA into 4'-phosphopantetheine. In contrast to pantetheine[21], 4'-phosphopantetheine was stable in serum, was taken up by cells via passive diffusion and was intracellularly re-converted into CoA. Via this route, exogenous CoA rescued CoA-deprived phenotypes at the cellular, developmental, organismal and behavioral level. We showed that CoA rescue was independent of the first three classic CoA biosynthetic steps (PANK, PPCS and PPCDC) and that it depended on the last bifunctional enzyme, COASY. Our data demonstrated the existence of an alternate mechanism for cells and organisms to influence intracellular CoA levels derived from an extracellular CoA source with 4'-phosphopantetheine as the key intermediate.

RESULTS

CoA supplementation rescues CoA-depleted phenotypes

In order to answer the question of whether cells are able to obtain CoA from sources other than classic *de novo* biosynthesis (Figure 1a), we first sought to determine whether extracellular sources of CoA could serve as a supply for intracellular CoA. For this, we used RNA interference to induce PANK (first enzymatic step) depletion to block the *de novo* biosynthesis route and to create a CoA-depleted phenotype. Subsequently the rescue potential of exogenous CoA was tested. PANK depletion by RNA interference in *Drosophila* cultured S2 cells (Figure 1b insert) was associated with a reduction in cell count (Figure 1b,c) and histone acetylation levels (Figure 1d-e), as previously demonstrated[4]. Addition of CoA to the medium of the cultured cells rescued the cell count in a concentration-dependent manner (Figure 1c) and restored the histone acetylation phenotype (Figure 1f). Next, we questioned whether this rescue also applied to other cell types and systems of impaired CoA biosynthesis. Treating *Drosophila* S2 cells with the chemical PANK inhibitor Hopantenate (HoPan)[22], also induced a decrease in cell count (Supplementary Results, Supplementary Figure 1a) and histone acetylation levels (Supplementary Figure 1b-c). This HoPan-induced phenotype was also rescued by direct supplementation of CoA to the medium of the cells (Supplementary Figure 1a,d). Next, we studied the effects of HoPan in mammalian HEK293 cells to address the possibility that the beneficial effects of exogenous CoA were insect cell-specific. When HEK293 cells were treated with HoPan, they showed a phenotype similar to *Drosophila* S2 cells, with decreased cell count and impaired histone acetylation. When CoA was added to the culture medium both the decreased cell count (Figure 1g) and the impaired histone acetylation phenotypes (Figure 1h) were rescued. These *in vitro* results confirmed the potency of exogenous CoA to rescue phenotypes induced by impaired PANK in diverse cellular systems.

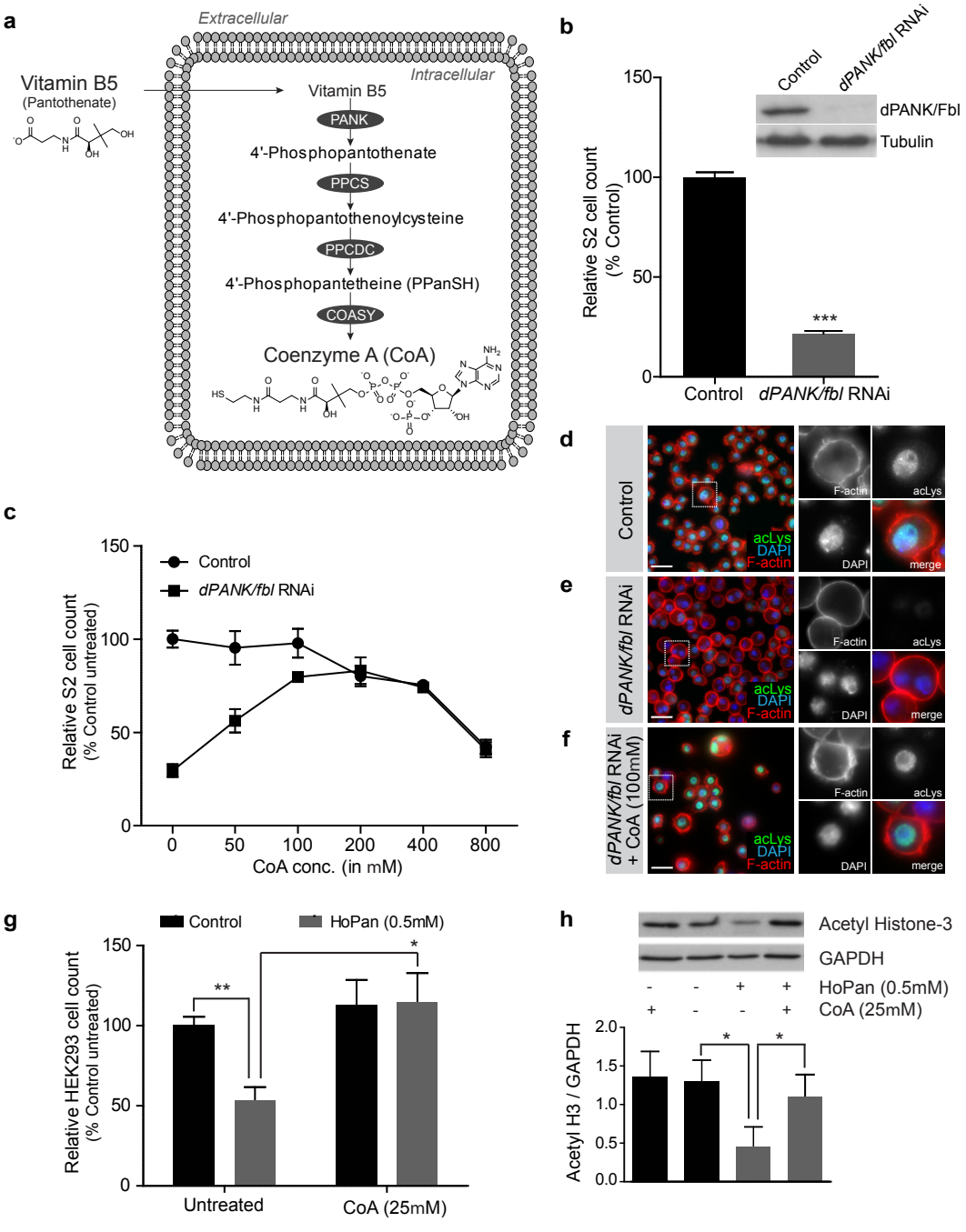

Figure 1: CoA supplementation rescues PANK impaired phenotypes. a. Canonical *de novo* CoA biosynthesis pathway. VitaminB5 (pantothenate) is taken up and intracellularly converted to CoA by the enzymes PANK, PPCS, PPCDC, and COASY. (PANK - Pantothenate Kinase; PPCS - Phosphopantothenoylcysteine synthetase; PPCDC - Phosphopantothenoylcysteine decarboxylase; COASY - CoA

synthase). **b**. Relative *Drosophila* S2 cell count of control (100%) and *dPANK/fbl* RNAi treated cells. 'Insert' - western blot of dPANK/Fbl protein levels in control and *dPANK/fbl* RNAi treated cells, tubulin as loading control. Data represent mean ± SD (n = 3), two-tailed unpaired Student's t-test was used (***P ≤ 0.001). **c**. Relative cell count of control (100%) and *dPANK/fbl* RNAi treated cells in the presence of increasing concentrations of CoA. Data represent mean ± SD (n = 4). **d-f**. Immunofluorescence showing protein acetylation levels in control (**d**) and *dPANK/fbl* RNAi treated cells without (**e**) and with CoA (**f**). Anti-acetylated-Lysine antibodies (green), Rhodamin-Phalloidin (red, F-actin) and DAPI (blue, DNA) were used. Scale bar indicates 20_m. **g**. Relative cell count of control (100%) and HoPan treated HEK293 cells with and without CoA. Data represent mean ± SD (n = 3), two-tailed unpaired Student's t-test was used (*P ≤ 0.05, **P ≤ 0.01). **h**. Western blot and quantification of histone acetylation levels in control and HoPan treated HEK293 cells in presence and absence of CoA. GAPDH was used as loading control. Data indicate mean ± SD (n = 3), two-tailed unpaired Student's t-test was used (*P ≤ 0.05).

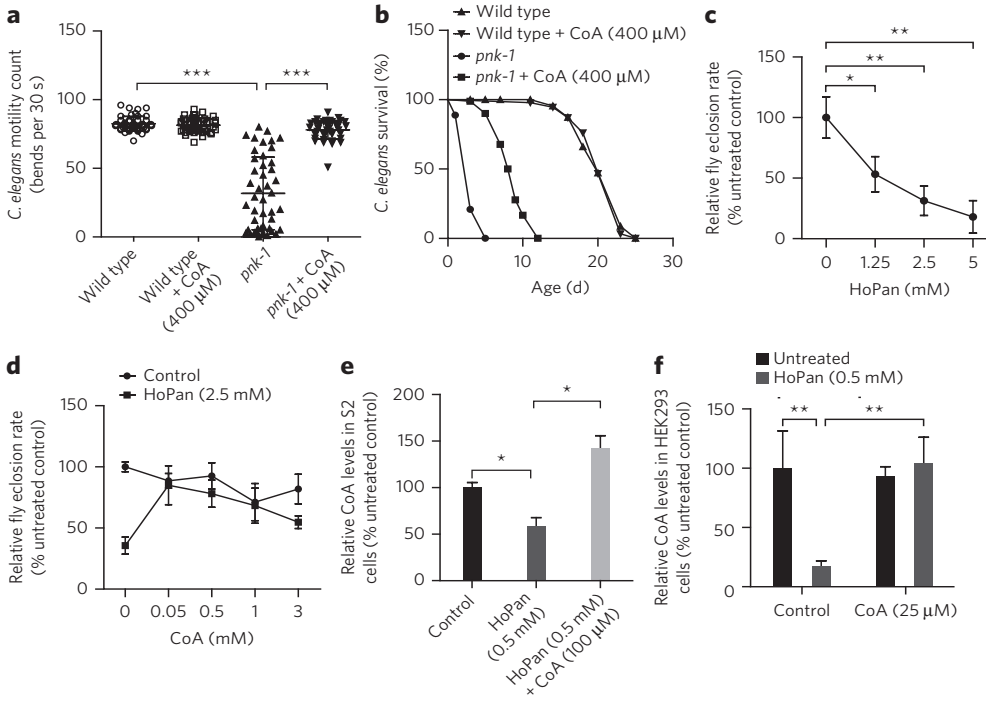

Figure 2: CoA rescues impaired PANK phenotypes of *C. elegans* and *Drosophila*. a. Motility (bends per 30 sec) was determined in *C. elegans pnk-1* mutants and wild-types with and without CoA treatment. Error bars indicate ± SD (n = 45), analysed with two-tailed unpaired Student's t-test (***P ≤ 0.001). **b**. Lifespan analysis of *C. elegans pnk-1* mutants with (n = 90) and without (n = 96) CoA treatment compared to wild-types with (n = 92) and without (n = 83) CoA treatment. Survival curves were significant (P < 0.001), analyzed with Log-rank (Mantel-Cox) test, between untreated and CoA treated *pnk-1* mutants. **c**. Eclosion rate of adult control flies (set as 100%) and flies treated with increasing concentrations HoPan, added to the food during development. Data indicates mean ± SD (n = 3), two-tailed unpaired Student's t-test was used (*P ≤ 0.05, **P ≤ 0.01). **d**. Relative eclosion rate of adult control flies and flies treated with 2.5mM HoPan, added to the food during development, in the presence of increasing concentrations of CoA. Data represent mean ± SD (n = 3). **e**. Intracellular CoA levels measured with HPLC in *Drosophila* S2 control cells (100%) and cells treated with HoPan alone or with HoPan and CoA. **f**. Intracellular CoA levels measured with HPLC in HEK293 control cells (100%) and HoPan treated cells with and without CoA. Data (in **e**,**f**) represent mean ± SD (n = 3), analysed with two-tailed unpaired Student's t-test (*P ≤ 0.05, **P ≤ 0.01).

To test the effect of CoA supplementation in vivo, we used homozygous Caenorhabditis elegans (C. elegans) pantothenate kinase (pnk-1) mutants4, which showed decreased motility (Figure 2a, Supplementary Figure 2a) and a decreased lifespan (Figure 2b). Addition of CoA to the food of these mutants improved these phenotypes significantly (Figure 2a,b and Supplementary Figure 2a-e). Furthermore, when a *Drosophila* w1118 control fly line was treated with HoPan, larval lethality was induced and a decreased eclosion (emerging from the pupal case) rate was observed (Figure 2c). This HoPan-induced phenotype was fully rescued by the addition of CoA to the food of the larvae (Figure 2d).

These data demonstrated that supplementation of CoA reverted the phenotypes arising from impaired *de novo* CoA biosynthesis, an effect that was observed in diverse eukaryotic cell types and organisms.

External supply of CoA influences intracellular CoA

The observed rescue effect could occur in several ways. Either intracellular CoA levels could have been restored, or rescue was achieved independent of the restoration of CoA levels in the cells. If the latter was true, intracellular levels of CoA would not be restored by exogenous CoA. To investigate this, a sensitive HPLC method was developed consisting of pre-column thiol-specific derivatization of samples with ammonium 7-fluorobenzofurazan-4-sulfonate (SBDF), followed by chromatographic separation by gradient elution on a C18 column and fluorescence detection (see online Methods). The HPLC-CoA analysis showed that intracellular CoA levels were significantly reduced in extracts of HoPan-treated S2 and HEK293 cells, addition of CoA to the culture medium restored the intracellular concentration of CoA (Figure 2e,f). These results suggested that extracellular CoA exerted its beneficial effects in CoA-depleted cells by increasing and thereby "normalizing" intracellular CoA concentrations.

In serum, CoA is degraded to stable 4'-phosphopantetheine

The mechanism behind this alternative CoA route was not known. The observations in Figure 1 and 2 indicated that either 1) CoA entered cells directly, although such a transport process has not been described; or 2) CoA was converted to an intermediate product that entered the cell and was converted back to CoA in a PANK-independent manner. Previous research found that CoA is not stable in liver extracts and degrades to 50% at -20°C after a week[23], however, the stability of CoA in an extracellular environment such as in aqueous or in standard cell culture medium is unknown. Moreover, these early reports did not identify specific degraded or converted products. We measured the stability of CoA in PBS, serum-free medium, medium containing fetal calf serum and in fetal calf serum (FCS) during a 3hrs incubation. HPLC analysis revealed that CoA was relatively stable in PBS and serum free medium, with >95% of the initial concentration still present after 3hrs (Supplementary Figure 3, 4a). However, in the presence of fetal calf serum, CoA was rapidly degraded (Figure 3a; Supplementary Figure 4b). After 3hrs of incubation only 10% of the initial concentration was detectable (Supplementary Figure 3, 4b). Detailed stability analysis at different time points in PBS and fetal calf serum revealed that 90% of CoA was already degraded after 30 min in fetal calf serum (Figure 3a). Disappearance of CoA coincided with the appearance of one unknown thiol-containing product in the HPLC chromatogram, which migrated at 18.273 minutes and remained stable over the time course of 3hrs (Figure 3b, Supplementary Figure 4b). Since this extra

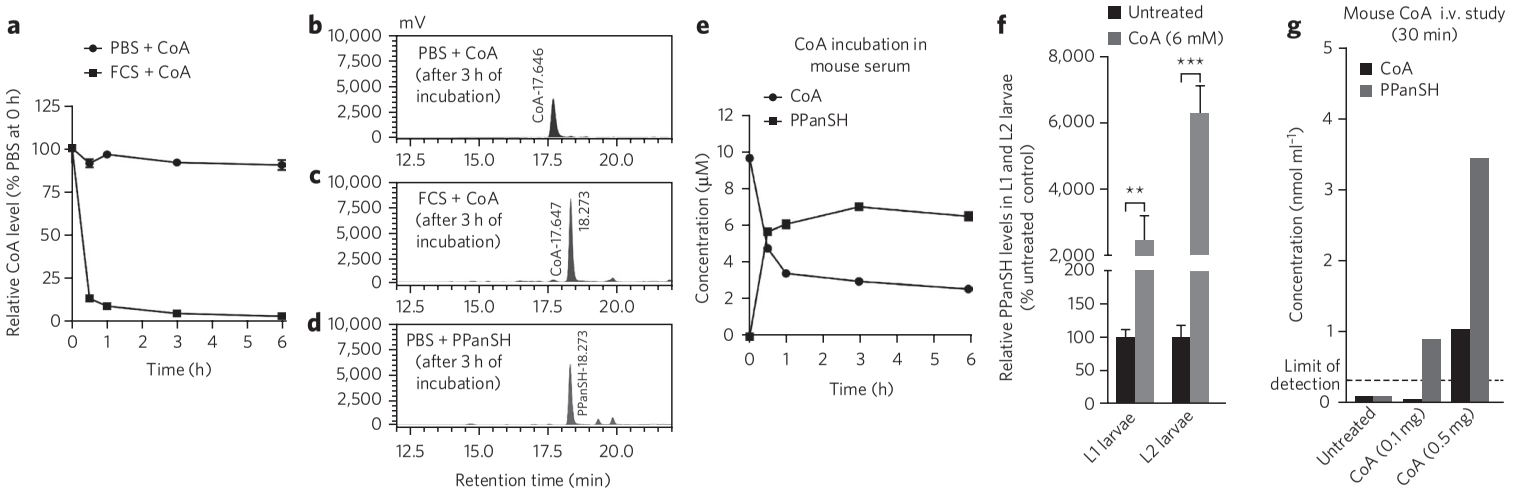

Figure 3: CoA is converted into stable 4'-phosphopantetheine (PPanSH) *in vitro,* in serum, and *in vivo* in *Drosophila* and mice. a. Stability profile of CoA determined by HPLC analysis in PBS (time 0 hrs in PBS is 100%) and in fetal calf serum over the course of 6 hrs. Data represent mean ± SD (n = 3). **b-c**. HPLC chromatogram profile of CoA incubated for 3 hrs in (**b**) PBS and in (**c**) fetal calf serum (FCS). (**d**) Retention time of standard PPanSH is identical to the observed conversion product of CoA in fetal calf serum. **e**. CoA was added to mouse serum and concentrations of CoA and PPanSH in mouse serum over 6 hrs were determined by HPLC analysis. Data indicate mean ± SD (n = 3). **f**. Relative PPanSH levels in *Drosophila* L1 and L2 stage larvae determined by HPLC analysis under untreated conditions (100%) and after feeding CoA. Data indicate mean ± SD (n = 3), two-tailed unpaired Student's t-test was used ($^{**}P \leq 0.01$, $^{***}P \leq 0.001$). **g**. Concentration of CoA and PPanSH in mouse serum determined by HPLC analysis, 30 min after *in vivo* injecting various amounts of CoA intravenously. Data represent mean (n = 2), in g; Solid thick bars without error bars indicate no PPanSH or CoA was detected.

peak had to be a thiol-containing molecule, we speculated that it could be a CoA degradation product, namely dephospho-CoA, 4'-phosphopantetheine (PPanSH), or pantetheine[2]. In contrast to dephospho-CoA and pantetheine, 4'-phosphopantetheine is not commercially available and hereto, we chemically synthesized this compound (Supplementary Note) in order to complete our analysis. HPLC analysis and comparison with standards demonstrated that the thiol-containing degradation product of CoA was neither dephospho-CoA nor pantetheine (Supplementary Figure 4a-e), but it exactly matched the retention time of 4'-phosphopantetheine standard (Figure 3c,d; Supplementary Figure 4b,c). These results indicated that CoA was converted into 4'-phosphopantetheine in serum and was stable. This is in contrast to pantetheine which is not stable in serum (Supplementary Figure 5a)[21]. We further investigated the conversion of CoA in mouse serum and in human serum. In sera from both species, including serum derived from PKAN patients (Supplementary Figure 5b) we found that CoA was also converted to 4'-phosphopantetheine (Figure 3e, Supplementary Figure 5c).

To investigate whether this conversion also occured *in vivo*, *Drosophila* larvae were fed CoA, and L1 and L2 stage larval extracts were obtained after 2 days and 3 days of feeding, respectively. HPLC analysis showed that externally added CoA resulted in increased levels of 4'-phosphopantetheine in both L1 (>20 fold) and L2 larvae (>60 fold) (Figure 3f). To investigate whether this conversion also occured in higher organisms, different concentrations of CoA were injected intravenously into adult mice, and plasma was collected after 30 min and 6 hrs. HPLC analysis in combination with mass spectrometry revealed the presence of low levels of endogenous 4'-phosphopantetheine in fresh mouse serum (Supplementary Figure 6a-c) and showed that the injected CoA was rapidly converted to 4'-phosphopantetheine after 30 min (Figure 3g). Moreover we demonstrated using mass spectrometry that elevated levels of 4'-phosphopantetheine were still present in the plasma 6 hrs after CoA injection (Supplementary Figure 6d).

These data indicated that CoA is converted into 4'-phosphopantetheine *in vitro* and *in vivo*. Furthermore these results suggested that 4'-phosphopantetheine could be the principal molecule that was taken up by CoA-depleted cells, converted back into CoA intracellularly and this resulted in rescue of the CoA-depleted phenotypes.

Conversion of CoA into 4'-phosphopantetheine by ENPPs

Next we questioned which factors could be responsible for the conversion of CoA into 4'-phosphopantetheine in serum. To identify candidate enzymes, serum from various species (fetal calf, mouse and human) was pre-conditioned, and CoA conversion into 4'-phosphopantetheine was assessed. First, the effect of heat inactivation of the serum was studied. HPLC analysis showed that heating the serum at 56°C for 30 min completely abolished the conversion of CoA to 4'-phosphopantetheine (Figure 4a), this indicated the involvement of enzymes or proteins in the process. Second, the conversion of CoA to 4'-phosphopantetheine requires the hydrolysis of a phosphoanhydride bond, which is typically catalyzed by (pyro)phosphatases or hydrolases. The majority of enzymes in the known family of (pyro)phosphatases and hydrolases depend on metal ions for their activity. To test these candidates, ethylenediaminetetraacetic acid (EDTA) was added to serum to chelate metal ions. Treatment of serum with EDTA completely prevented the formation of 4'-phosphopantetheine (Figure 4b). This strongly

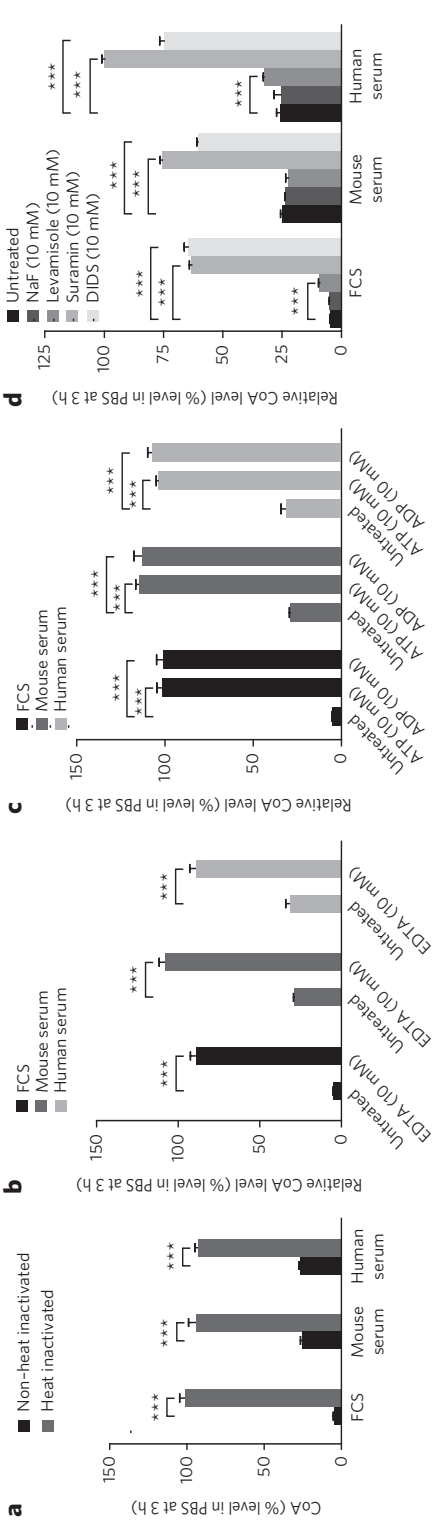

Figure 4: Conversion of CoA into stable 4'-phosphopantetheine (PPanSH) in serum is mediated by heat unstable and metal-activated enzymes. a CoA was incubated in heat-inactivated fetal calf serum, mouse serum and human serum for 3 hrs and CoA stability was measured using HPLC analysis. **b** CoA stability was determined in fetal calf serum, mouse serum and human serum pre-treated with EDTA (10mM) and CoA levels were measured after 3 hrs using HPLC analysis. **c** CoA was incubated in fetal calf serum, mouse serum and human serum pre-treated with ATP or ADP (both 10mM) and CoA levels were measured after 3 hrs. **d** CoA stability was determined in fetal calf serum, mouse serum and human serum pre-treated with sodium fluoride (NaF), levamisole, suramin or 4,4'-diisothiocyanatostilbene-2,2' disulphonic acid (DIDS) (all 10mM) and CoA levels were measured after 3 hrs. Data in all the above represent mean ± SD (n = 3), two-tailed unpaired Student's t-test was used for statistical analysis to compare indicated subsets (* $P \leq 0.05$, ** $P \leq 0.01$, *** $P \leq 0.001$). In all the above experiments CoA was added to the indicated sera to a final concentration of 10μM, and percentages relative to CoA stability for 3 hrs in PBS (100%) are indicated (see Online methods for detailed protocol).

suggested that metal ions were required for the CoA conversion. The most likely hydrolase or (pyro) phosphatase candidates, which possess the ability to convert CoA and which are metal-ion dependent for their activity, are nudix hydrolases, alkaline phosphatases and ecto-nucleotide pyrophosphatases (ENPPs)[24-28]. These candidate enzymes are also known for their ability to hydrolyze adenosine 5'-triphosphate (ATP) and adenosine 5'-diphosphate (ADP)[29-31]. Therefore, we tested the conversion of CoA into 4'-phosphopantetheine in serum after addition of excess ATP and ADP. Both competitively blocked the conversion in all sera tested, further underscoring the involvement of one of these enzymes (Figure 4c). Alkaline phosphatase and ENPPs are excreted by cells and are present in serum[29, 32]. Nudix hydrolases are intracellular hydrolases of CoA[25, 30]; however, an additional possible extracellular role for this class of hydrolases cannot be excluded.

Next, we used sodium fluoride (NaF), and levamisole to inhibit nudix hydroloases, and alkaline phosphatase respectively, and in addition, we also used two different ENPP inhibitors, suramin and 4,4'-diisothiocyanatostilbene-2,2' disulphonic acid (DIDS)[33-35]. Our data showed that only suramin and DIDS were able to efficiently abolish the degradation of CoA into 4'-phosphopantetheine in all the sera, unlike levamisole, and sodium fluoride (NaF) which showed only mild or no inhibition of CoA degradation into 4'-phosphopantetheine, respectively (Figure 4d). Sodium fluoride (NaF) did not influence CoA degradation in serum, which indicated that either nudix hydrolases were not present or did not degrade CoA in serum. These experiments implicated ENPPs as the most likely class of enzymes to hydrolyze CoA into 4'-phosphopantetheine in serum. Moreover, in all of the CoA serum stability experiments listed above, there was an inverse correlation between the levels of CoA and 4'-phosphopantetheine (Supplementary Figure 7a-c), which underscored that CoA degradation into 4'-phosphopantetheine was mediated by ENPPs.

4'-phosphopantetheine rescues CoA-depleted phenotypes

Our data so far predicted that PANK impairment not only induced decreased CoA levels but also decreased levels of 4'-phosphopantetheine. Furthermore, it predicted that addition of 4'-phosphopantetheine to CoA-depleted cells could rescue the induced phenotypes. HPLC analysis of HoPan treated *Drosophila* S2 cells indeed showed reduced levels of 4'-phosphopantetheine, and external supplementation with either CoA or 4'-phosphopantetheine significantly increased intracellular levels of 4'-phosphopantetheine (Figure 5a). Moreover, when 4'-phosphopantetheine was added to *Drosophila* S2 cells treated with HoPan (Figure 5b) or *dPANK/fbl* RNAi (Figure 5c) the CoA-depleted phenotype was again rescued. 4'-Phosphopantetheine supplementation also rescued the histone acetylation defect in *Drosophila* S2 cells treated with *dPANK/fbl* RNAi (Supplementary Figure 8a-c) or HoPan (Supplementary Figure 8d-f). Finally, we tested the rescue effect of 4'-phosphopantetheine in HoPan-treated mammalian HEK293 cells and found that it also rescued the HoPan-induced reduction in cell count (Supplementary Figure 8g), intracellular CoA levels (Supplementary Figure 8h) and histone acetylation levels (Supplementary Figure 8i). Next we investigated whether intact 4'-phosphopantetheine entered cells and whether it was subsequently converted into CoA. First we treated intact cultured *Drosophila* S2 cells with stable isotope-labelled 4'-phosphopantetheine under various conditions, and mass spectrometry analysis was used to

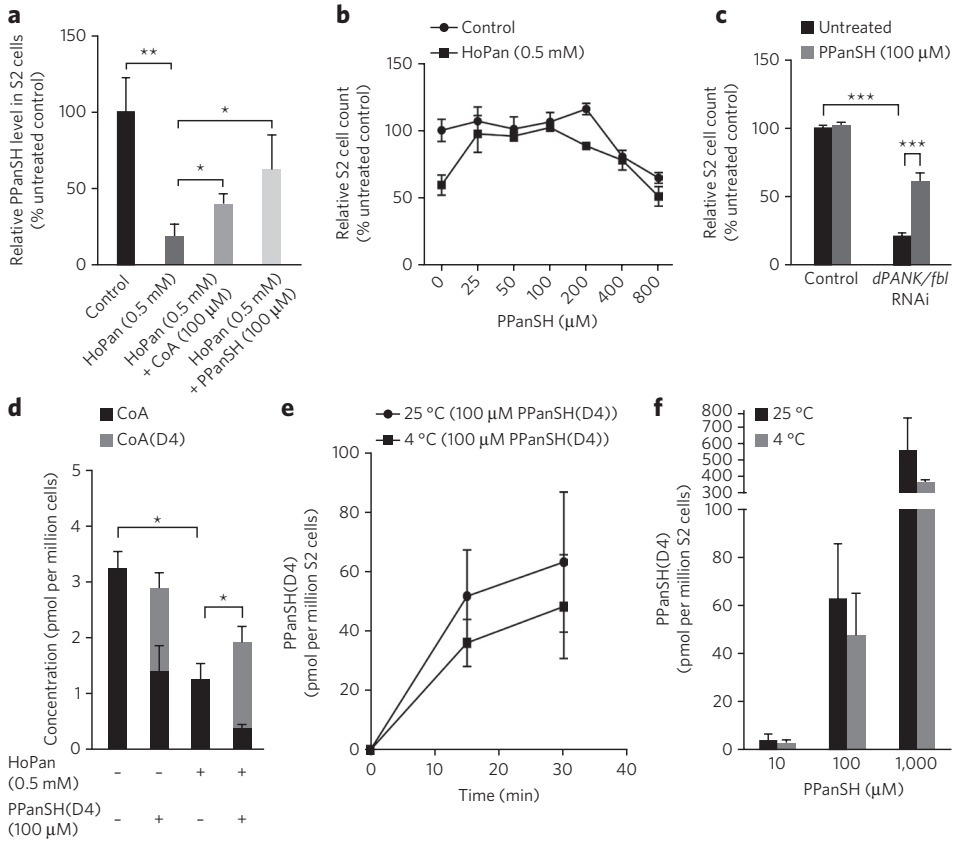

Figure 5: External supplementation of 4'-phosphopantetheine (PPanSH) rescues CoA-deprived phenotypes. a. Measurement of intracellular PPanSH levels by HPLC analysis in control *Drosophila* S2 cells (100%) and cells treated with HoPan (0.5mM) with and without addition of CoA or PPanSH (100μM). **b**. *Drosophila* S2 cell count was determined in control cells (100%) and HoPan (0.5mM) treated cells under conditions of increasing PPanSH concentrations. **c**. Cell count was determined in control (100%) and *dPANK/fbl* RNAi treated *Drosophila* S2 cells with an without addition of PPanSH (100μM) to the medium. **d**. S2 cells, with and without HoPan (0.5mM) were incubated with stable-isotope labelled PPanSH(D4) (100μM) and levels of both unlabeled CoA and labelled CoA(D4) were measured using mass spectrometry. Cumulative CoA and CoA(D4) levels were used for statistical analysis. **e**. Stable-isotope labelled PPanSH(D4) (100μM) was added to S2 cells at 4°C and 25°C, incubated for various time intervals and mass spectrometry was used to measure levels of labelled compound in harvested cell extracts. **f**. Stable-isotope labelled PPanSH(D4) (10, 100, 1000μM) was added to S2 cells for 30min and mass spectrometry was used to measure levels of labelled compound in harvested cell extracts. Data in all the above represent mean ± SD (n = 3), two-tailed unpaired Student's t-test was used for statistical analysis to compare indicated subsets ($^{*}P \leq 0.05$, $^{**}P \leq 0.01$, $^{***}P \leq 0.001$).

measure the levels of stable isotope-labelled CoA and 4'-phosphopantetheine (Supplementary Figure 9a-d) within the harvested cell extracts. When labelled 4'-phosphopantetheine is added to the cell culture medium, labelled CoA was detected in harvested cell extracts (Figure 5d). In the presence of HoPan, CoA levels were decreased and replenished in the form of labelled CoA when labelled 4'-phosphopantetheine was added. These data demonstrated that exogenously provided 4'-phosphopantetheine was able to enter cells and intracellularly converted into CoA under normal culturing conditions and under

conditions of impaired CoA biosynthesis by HoPan. Next we investigated the characteristics of the passage of 4'-phosphopantetheine over the cell membrane. First, within 30 min after the incubation of cells with labelled 4'-phosphopantetheine, the intracellular presence of labelled 4'-phosphopantetheine was detected in cells cultured at 25°C (normal culturing temperature of S2 cells) and 4°C. There was no significant difference in the intracellular levels of labelled 4'-phosphopantetheine between these two conditions (Figure 5e). Next we investigated whether under these conditions, the levels of intracellular 4'-phosphopantetheine increased to the same extent as the externally added increased concentrations of 4'-phosphopantetheine. Hereto an increasing concentration series (10-100-1000μM) of labelled 4'-phosphopantetheine was added to the cells. This appeared to be the case (Figure 5f). These results indicated that the capacity of cells to accumulate the externally provided 4'-phosphopantetheine was not influenced by temperature and was determined by extracellularly provided concentrations. Finally we investigated the membrane permeating efficiency of 4'-phosphopantetheine using a Parallel Artificial Membrane Permeability Assay (PAMPA assay)36. Based on this assay 4'-phosphopanteheine but not CoA showed membrane permeating properties (Supplementary Figure 9e-f). Altogether, these results pointed to a capacity of 4'-phosphopanteheine to permeate membranes via passive diffusion.

CoA rescues *dPANK/fbl, dPPCDC* but not *dCOASY* phenotypes

Our data showed that CoA from external sources can replenish intracellular CoA levels through its hydrolysis product 4'-phosphopantetheine and subsequent conversion back to CoA. The most likely candidate for the latter conversion is the last bifunctional enzyme, COASY, of the classic CoA biosynthetic pathway. This hypothesis (Supplementary Figure 10) predicts that CoA but not Vitamin B5 can rescue phenotypes caused by mutations in genes encoding enzymes upstream of 4'-phosphopantetheine in the CoA pathway. As a corollary, CoA would not be predicted to rescue *COASY* mutant phenotypes.

We aimed to test this hypothesis. In the genome of *Drosophila* single orthologs were identified for all the enzymes involved in CoA biosynthesis[12], including *dPANK/fbl*, *dPPCDC* and *dCOASY*. A set of *Drosophila* strains was obtained, carrying either mutations in genes encoding these enzymes or carrying a UAS-RNAi construct. Homozygous mutants or flies ubiquitously expressing the RNAi construct showed a downregulation of mRNA levels (Supplementary Figure 11a-c) or protein levels (Supplementary Figure 12a) of these enzymes. CoA and 4'-phosphopantetheine levels were also significantly reduced in all conditions (Supplementary Figure 12b-e), with the exception of *dCOASY* mutants, which showed a significant reduction of CoA, but not 4'-phosphopantetheine (Supplementary Figure 12f).

It should be stressed that not all mutants with defects in CoA biosynthesis enzymes showed an identical phenotype, which can be explained by the type of flylines (RNAi expressing lines, hypomorphic or null mutants) used. This has been reported previously not only for *Drosophila* but also for other organisms[12, 37]. Regardless of the severity and developmental stage in which the phenotypes manifested, the determination of the rescue potential of CoA in the available mutants was a valuable tool to test our hypothesis. A scheme of the hypothesis, *Drosophila* life span and the phenotypes of the used fly lines are presented in Supplementary Figure 10.

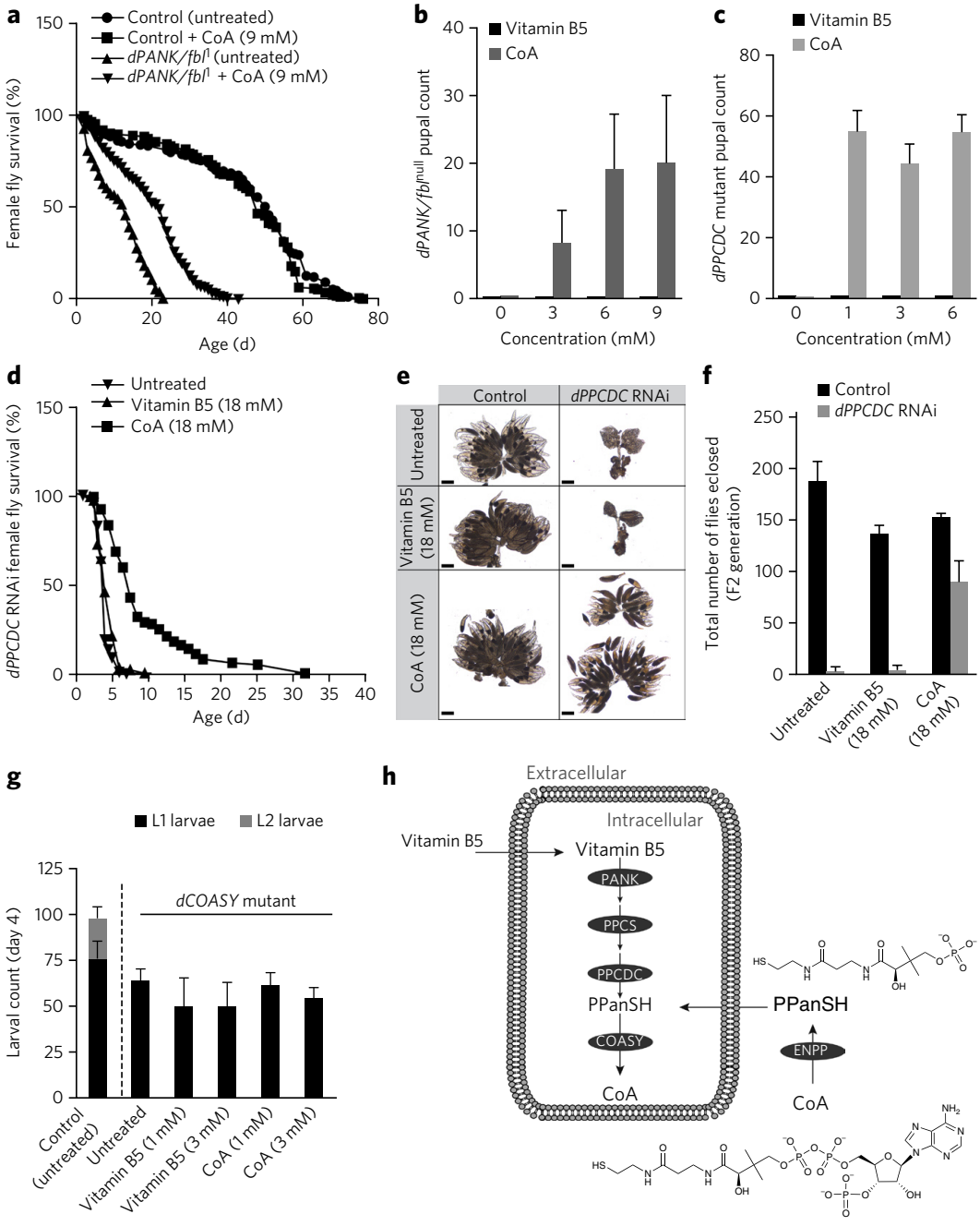

Figure 6: External supplementation of CoA rescues *dPANK/fbl- and dPPCDC*- but not *COASY*-impaired phenotypes.

a. Lifespan analysis of *dPANK/fbl*^{1} mutants with (n = 260) or without (n = 207) CoA treatment, compared with control flies with (n = 175) or without (n = 176) CoA treatment. Survival curves were significant with Log-rank (Mantel-Cox) test, between untreated and CoA (9mM) treated *dPANK/fbl*^{1} mutants (P value < 0.001). **b**. Number of pupae of *dPANK/fbl*^{null} mutants after treatment of increasing concentrations of CoA or Vitamin B5. **c**. Number of pupae of *dPPCDC* mutants untreated or after treatment with CoA or Vitamin B5. **d**. Lifespan analysis of the *dPPCDC* RNAi line untreated (n = 111), treated with CoA (n = 102) or Vitamin B5 (n = 102). Survival curves

were significant with Log-rank (Mantel-Cox) test, between untreated and CoA (18mM) treated *dPPCDC* RNAi flies (P value < 0.001).**e**. Ovarian size of control and *dPPCDC* RNAi expressing *Drosophila* females, untreated or treated with CoA or Vitamin B5, imaged with light microscopy. Scale bar = 200_m. **f**. Amount of eclosed adult progeny of *dPPCDC* RNAi females, crossed with control males raised on control food or supplemented with CoA or Vitamin B5. **g**. Amount of L1 and L2 *dCOASY* mutant larvae and controls untreated or treated with CoA or Vitamin B5. **h**. Proposed non-canonical CoA supply route starting with extracellular CoA. ENPPs is ecto-nucleotide pyrophosphatases. Data represents mean ± SD (n = 3) in b,c,f,g; Solid thick bars without error bars indicate no pupae or eclosed flies observed.

We first tested 2 available mutants for *dPANK/fbl*; the hypomorphic[19] *dPANK/fbl*^{1} and the null mutant *dPANK/fbl*^{null}. Homozygous *dPANK/fbl*^{1} mutants showed reduced levels of dPANK/Fbl protein, and in homozygous *dPANK/fbl*^{null} mutants, levels of dPANK/Fbl protein were below detection (Supplementary Figure 12a). Correlating with this, homozygous *dPANK/fbl*^{1} mutants showed a reduced adult lifespan (Figure 6a, Supplementary Figure 13a)[12, 19], while homozygous *dPANK/fbl*^{null} mutants only developed until an early L2 larval stage and pupae were not observed (Figure 6b). Addition of CoA to the food of the homozygous *dPANK/fbl*^{1} mutants increased the life span from 20 to 40 days (Figure 6a, Supplementary Figure 13a), and CoA addition to the food of homozygous *dPANK/fbl*^{null} mutants extended development from the L2 stage to early pupal development (Figure 6b). These results supported our hypothesis. Remarkably, in dPANK/fbl^{null} mutants low CoA and 4'-phosphopantetheine levels were detected (Supplementary Figure 12c). This may come from a maternal supply or the flyfood as possible resources (Supplementary Figure 13b).

To compromise dPPCDC, the enzyme carrying out the third step of the CoA biosynthesis pathway, we used a UAS-RNAi line ('*dPPCDC* RNAi') as well as a *dPPCDC* mutant and investigated rescue by CoA. Homozygous *dPPCDC* mutants showed lethality at early second instar larval stage L2 (Figure 6c). *dPPCDC* RNAi expressing flies showed a milder phenotype, where adult flies were viable but showed a reduced lifespan (Figure 6d). Females also showed sterility associated with small ovaries and no eggs were produced (Figure 6e, Supplementary Figure 14a-d). Addition of CoA to the food of homozygous *dPPCDC* mutants extended larval development to late pupal stage (Figure 6c). For the *dPPCDC* RNAi expressing flies, supplementation of CoA to the food increased the maximal lifespan from 10 days to 30 days (Figure 6d, Supplementary Figure 14e). In addition, female sterility was rescued based on the observations of egg production and eclosion of viable offspring (Figure 6e,f, Supplementary Figure 14c-d). These results were also consistent with our hypothesis.

Finally we tested a mutant line of the bifunctional enzyme dCOASY, downstream of 4'-phosphopantetheine. Homozygous *dCOASY* mutants developed until first instar larval stage and addition of CoA to the food did not result in a significant rescue (Figure 6g). As a negative control for all rescue experiments, vitamin B5 was added to the food, and this did not result in any significant rescue of the phenotypes. A summary of the rescue with CoA in all flylines is presented in Supplementary Figure 10.

To test our hypothesis further, *COASY* was downregulated with RNAi in mammalian HEK293 cells. Under these conditions levels of COASY protein, CoA and histone acetylation were significantly reduced (Supplementary Figure 14g-f). As in *dCOASY* mutants, levels of 4'-phosphopantetheine remained

unaltered in COASY-compromised mammalian cells (Supplementary Figure 14g). Addition of CoA to the medium neither rescued the *COASY* RNAi-induced decrease in intracellular CoA levels (Supplementary Figure 14g) nor restored histone acetylation levels (Supplementary Figure 14f). These results were also in agreement with our hypothesis.

Taken together, these results demonstrated that impairment of the CoA biosynthetic pathway by genetic manipulation can give rise to highly complex pleiotropic effects affecting lifespan, development and fecundity. These phenotypes can be (partially) rescued by the addition of CoA to the food of the animals, which is then hydrolyzed to 4'-phosphopantetheine which crosses the plasma membrane via passive diffusion before being converted back to CoA intracellularly, a step requiring COASY (Figure 6h).

DISCUSSION

In our study we addressed the basic question of whether cells and organisms possess alternative ways to obtain the essential molecule CoA in addition to the canonical pathway utilizing Vitamin B5. We demonstrate that cells and organisms are able to acquire exogenous CoA, which is converted into the stable molecule 4'-phosphopantetheine, which enters cells and is converted again into CoA. These newly identified characteristics of 4'-phosphopantetheine suggest that this molecule can serve as a transport form of CoA or stable reservoir for rapid access and conversion. The proposed mechanism hypothetically allows a net flow of CoA or 4'-phosphopantetheine between cells and between membrane-bound cellular compartments. Our data further suggest that not all cells or organelles within an organism need to harbor all CoA biosynthetic enzymes in order to obtain CoA and that the route to CoA does not necessarily need to follow the archetypal direction starting from the uptake of Vitamin B5. Moreover, these observations hold promise for therapeutic intervention for PKAN because 4'-phosphopantetheine is stable in serum and passes through cell membranes, thereby allowing for restoration of intracellular CoA levels in cells with defective CoA synthesis. The stability of 4'-phosphopantetheine is in strong contrast to characteristics of the dephosphorylated form, pantetheine, which is degraded rapidly in serum by pantetheinases into vitamin B5 and cysteamine[20, 21]. These results show that the phosphate group protects the molecule from degradation and allows 4'-phosphopantetheine to serve as an effective substrate for CoA biosynthesis from its ready reserve in the circulation.

One intriguing question is whether the proposed route shown here has a physiological function or whether it is artificially provoked by manipulating concentrations of extracellular CoA. Compared to CoA concentrations in cytoplasm [0,02-0,14 mM] and mitochondria [2,2-5 mM][38], the concentrations used in our study (_M range) are relatively low. Answers may come from previous studies demonstrating that bacteria are able to excrete, but not take up 4'-phosphopantetheine from their environment, suggesting that bacteria-derived 4'-phosphopantetheine may be present in the digestive system[39]. The presence of endogenous 4'-phosphopantetheine in mouse serum and in dPANK/fbl^{null} mutants are consistent with a possible source of extracellular 4'-phosphopantetheine. The function of such a 'ready' pool of CoA-precursor may be for transport from one organ to another. In addition to being a source for intracellular

CoA, extracellular CoA or 4'-phosphopantetheine may have signaling functions based on reports of an effect of CoA on platelet aggregation and vasoconstriction[40, 41]. Our results suggest that these effects, which have been attributed to CoA, may in fact be from 4'-phosphopantetheine. Future experiments are required to demonstrate the presence and possible impact of a net flow of CoA between organelles, cells and organisms (such as between intestine bacteria to the host).

The ability of 4'-phosphopantetheine to translocate across membranes answers long-standing questions regarding the intracellular distribution of CoA and its biosynthetic enzymes. CoA is present in the cytoplasm and in organelles including mitochondria[38]. All CoA biosynthetic enzymes are present in cytoplasm[42] but only a subset have been found in mitochondria. It remains unclear how mitochondria obtain CoA, and the localization of COASY (but not the other CoA biosynthetic enzymes) to the mitochondrial matrix, is also unexplained[17, 43]. It has been postulated that CoA synthesized in the cytosol can be transported into the mitochondrial matrix by specific CoA transporters localized in the mitochondrial inner membrane[44]. Indeed evidence for the presence of such CoA transporters has been presented[45]. Based on our observations we hypothesize that 4'-phosphopantetheine is able to passage over the mitochondrial inner membrane into the matrix and be subsequently converted into CoA by matrix COASY. This may explain the localization of COASY in the mitochondrial matrix[17, 43].

The presence of a 4'-phosphopantetheine uptake mechanism may have large public health implications. Pathogens and parasites acquire resistance to current treatments, and species-specific inhibitors of CoA biosynthetic enzymes are attractive candidates for a new class of antibiotics and anti-malarial drugs[46, 47]. Such inhibitors may be more effective anti-microbials when 4'-phosphopantetheine uptake is blocked as well. Alternatively, differences in the uptake capacity of 4'-phosphopantetheine by eukaryotic cells (this manuscript) and bacteria[39] may be further explored as possible targets for antimicrobial strategies.

CoA is essential for coordinating key aspects of cell function. It is therefore not surprising that an extracellular pool exists to facilitate swift replenishment and that it relies on the formation of a stable intermediate. While these novel observations raise many new questions about CoA metabolism, they also suggest therapeutic approaches for a range of life-threatening human diseases.

ACKNOWLEDGEMENTS

This work was supported by the European Commission's Seventh Framework Programme [grant number FP7/2007-2013, HEALTH-F2-2011, grant agreement number 277984, TIRCON] to V.T., H.P, S.H., and O.C.M.S., by a GUIDE research school grant to B. S., a VICI grant to O.S (NWO-grant 865.10.012), a grant to V.T. of Telethon GGP11088. Part of the work has been performed at the UMCG Microscopy and Imaging Center (UMIC), which is sponsored by NWO-grant 175-010-2009-023. We thank Pieter G. Tepper and Ronald Van Merkerk (Pharmaceutical Biology, University of Groningen) for providing HPLC technical assistance and Jan-Willem Kok and Dick Hoekstra (Department of Cell Biology, UMCG) for helpful discussions. We also thank Theo de Boer and Freddy Oostebring from the Analytical Biochemical Laboratory BV (ABL, Assen, The Netherlands) for mass spectrometry analysis. We are grateful to PKAN patients and their families who contributed samples to this study.

AUTHOR CONTRIBUTIONS

B.S., M.B., R.A.L., G.K., H.P., S.H., V.T., and O.C.M.S. designed the research. B.S., M.B., M.v.d.Z., B.K., C.C., R.A.L., O.S., A.P. and N.A.G., performed experiments. B.S., M.B., R.A.L. and O.C.M.S. analyzed results. E.N., G.K., H.P., S.H., V.T., D.R., N.A.G. and O.C.M.S. supervised the research. B.S., N.A.G. and O.C.M.S. wrote the manuscript.

COMPETING FINANCIAL INTEREST

Declaration of competing financial interest: B.S., O.C.M.S., G.K., H.P., and A.P. are co-inventors on European patent application EP 2 868 662 A1. B.S.; O.C.M.S., G.K., and H.P. are co-inventors on the Slovenian patent application P-201400452. B.S.; O.C.M.S., G.K., H.P., S.H. are co-inventors on a patent application (soon to be filed). H.P. and G.K. are shareholders in Acies Bio, Ltd.

REFERENCES

1. Baddiley, J., Thain, E.M., Novelli, G.D. & Lipmann, F. Structure of coenzyme A. *Nature* **171**, 76 (1953).
2. Strauss, E. 7.11 - Coenzyme A Biosynthesis and Enzymology, in *Comprehensive Natural Products II*. (eds. H.-W. Liu & L. Mander) 351-410 (Elsevier, Oxford; 2010).
3. Shi, L. & Tu, B.P. Acetyl-CoA induces transcription of the key G1 cyclin CLN3 to promote entry into the cell division cycle in Saccharomyces cerevisiae. *Proceedings of the National Academy of Sciences of the United States of America* **110**, 7318-7323 (2013).
4. Siudeja, K. *et al.* Impaired Coenzyme A metabolism affects histone and tubulin acetylation in Drosophila and human cell models of pantothenate kinase associated neurodegeneration. *EMBO molecular medicine* **3**, 755-766 (2011).
5. Takahashi, H., McCaffery, J.M., Irizarry, R.A. & Boeke, J.D. Nucleocytosolic acetyl-coenzyme a synthetase is required for histone acetylation and global transcription. *Molecular cell* **23**, 207-217 (2006).
6. Choudhary, C. *et al.* Lysine acetylation targets protein complexes and co-regulates major cellular functions. *Science* **325**, 834-840 (2009).
7. Eisenberg, T. *et al.* Nucleocytosolic depletion of the energy metabolite acetyl-coenzyme a stimulates autophagy and prolongs lifespan. *Cell metabolism* **19**, 431-444 (2014).
8. Marino, G. *et al.* Regulation of autophagy by cytosolic acetyl-coenzyme A. *Molecular cell* **53**, 710-725 (2014).
9. McCoy, F. *et al.* Metabolic activation of CaMKII by coenzyme A. *Molecular cell* **52**, 325-339 (2013).
10. Srinivasan, B. & Sibon, O.C. Coenzyme A, more than 'just' a metabolic cofactor. *Biochemical Society transactions* **42**, 1075-1079 (2014).
11. Hoagland, M.B. & Novelli, G.D. Biosynthesis of coenzyme A from phospho-pantetheine and of pantetheine from pantothenate. *The Journal of biological chemistry* **207**, 767-773 (1954).
12. Bosveld, F. *et al.* De novo CoA biosynthesis is required to maintain DNA integrity during development of the Drosophila nervous system. *Human molecular genetics* **17**, 2058-2069 (2008).
13. Daugherty, M. *et al.* Complete reconstitution of the human coenzyme A biosynthetic pathway via comparative genomics. *The Journal of biological chemistry* **277**, 21431-21439 (2002).
14. Kupke, T., Hernandez-Acosta, P. & Culianez-Macia, F.A. 4'-phosphopantetheine and coenzyme A biosynthesis in plants. *The Journal of biological chemistry* **278**, 38229-38237 (2003).
15. Zhyvoloup, A. *et al.* Molecular cloning of CoA Synthase. The missing link in CoA biosynthesis. *The Journal of biological chemistry* **277**, 22107-22110 (2002).
16. Shimizu, S., Kubo, K., Tani, Y. & Ogata, K. Purification and Properties of Pantothenate Kinase from Brevibacterium ammoniagenes IFO 12071. *Bioscience, biotechnology, and biochemistry* **37**, 2863-2870 (1973).
17. Dusi, S. *et al.* Exome sequence reveals mutations in CoA synthase as a cause of neurodegeneration with brain iron accumulation. *American journal of human genetics* **94**, 11-22 (2014).
18. Zhou, B. *et al.* A novel pantothenate kinase gene (PANK2) is defective in Hallervorden-Spatz syndrome. *Nature genetics* **28**, 345-349 (2001).
19. Rana, A. *et al.* Pantethine rescues a Drosophila model for pantothenate kinase-associated neurodegeneration. *Proceedings of the National Academy of Sciences of the United States of America* **107**, 6988-6993 (2010).
20. Brunetti, D. *et al.* Pantethine treatment is effective in recovering the disease phenotype induced by ketogenic diet in a pantothenate kinase-associated neurodegeneration mouse model. *Brain : a journal of neurology* **137**, 57-68 (2014).
21. Wittwer, C.T., Gahl, W.A., Butler, J.D., Zatz, M. & Thoene, J.G. Metabolism of pantethine in cystinosis. *The Journal of clinical investigation* **76**, 1665-1672 (1985).
22. Zhang, Y.M. *et al.* Chemical knockout of pantothenate kinase reveals the metabolic and genetic program responsible for hepatic coenzyme A homeostasis. *Chemistry & biology* **14**, 291-302 (2007).
23. Shibata, K., Nakai, T. & Fukuwatari, T. Simultaneous high-performance liquid chromatography determination of coenzyme A, dephospho-coenzyme A, and acetyl-coenzyme A in normal and pantothenic acid-deficient rats. *Analytical biochemistry* **430**, 151-155 (2012).
24. Novelli, G.D., Schmetz, F.J., Jr. & Kaplan, N.O. Enzymatic degradation and resynthesis of coenzyme A. *The Journal of biological chemistry* **206**, 533-545 (1954).
25. Reilly, S.J., Tillander, V., Ofman, R., Alexson, S.E. & Hunt, M.C. The nudix hydrolase 7 is an Acyl-CoA diphosphatase involved in regulating peroxisomal coenzyme A homeostasis. *Journal of biochemistry* **144**, 655-663 (2008).
26. Shibata, K., Gross, C.J. & Henderson, L.M. Hydrolysis and absorption of pantothenate and its coenzymes in the rat small intestine. *The Journal of nutrition* **113**, 2107-2115 (1983).
27. Skrede, S. The degradation of CoA: subcellular localization and kinetic properties of CoA- and dephospho-CoA pyrophosphatase. *European journal of biochemistry / FEBS* **38**, 401-407 (1973).
28. Trams, E.G., Stahl, W.L. & Robinson, J. Formation of S-acyl pantetheine from acyl-coenzyme A by plasma membranes. *Biochimica et biophysica acta* **163**, 472-482 (1968).
29. Fernandez, N.J. & Kidney, B.A. Alkaline phosphatase: beyond the liver. *Veterinary clinical pathology / American Society for Veterinary Clinical Pathology* **36**, 223-233 (2007).
30. McLennan, A.G. The Nudix hydrolase superfamily. *Cellular and molecular life sciences : CMLS* **63**, 123-143 (2006).
31. Rucker, B. *et al.* Biochemical characterization of ecto-nucleotide pyrophosphatase/phosphodiesterase (E-NPP, E.C. 3.1.4.1) from rat heart left ventricle. *Molecular and cellular biochemistry* **306**, 247-254 (2007).
32. Jansen, S. *et al.* Structure of NPP1, an ectonucleotide pyrophosphatase/phosphodiesterase involved in tissue

calcification. *Structure* **20**, 1948-1959 (2012).

34. Grobben, B. *et al.* Ecto-nucleotide pyrophosphatase modulates the purinoceptor-mediated signal transduction and is inhibited by purinoceptor antagonists. *British journal of pharmacology* **130**, 139-145 (2000).
35. Gu, X. *et al.* A new fluorometric turn-on assay for alkaline phosphatase and inhibitor screening based on aggregation and deaggregation of tetraphenylethylene molecules. *The Analyst* **138**, 2427-2431 (2013).
36. Mensch, J. *et al.* Evaluation of various PAMPA models to identify the most discriminating method for the prediction of BBB permeability. *European journal of pharmaceutics and biopharmaceutics : official journal of Arbeitsgemeinschaft fur Pharmazeutische Verfahrenstechnik e.V* **74**, 495-502 (2010).
37. Rubio, S., Whitehead, L., Larson, T.R., Graham, I.A. & Rodriguez, P.L. The coenzyme a biosynthetic enzyme phosphopantetheine adenylyltransferase plays a crucial role in plant growth, salt/osmotic stress resistance, and seed lipid storage. *Plant physiology* **148**, 546-556 (2008).
38. Horie, S., Isobe, M. & Suga, T. Changes in CoA pools in hepatic peroxisomes of the rat under various conditions. *Journal of biochemistry* **99**, 1345-1352 (1986).
39. Jackowski, S. & Rock, C.O. Metabolism of 4'-phosphopantetheine in Escherichia coli. *Journal of bacteriology* **158**, 115-120 (1984).
40. Davaapil, H., Tsuchiya, Y. & Gout, I. Signalling functions of coenzyme A and its derivatives in mammalian cells. *Biochemical Society transactions* **42**, 1056-1062 (2014).
41. Manolopoulos, P. *et al.* Acyl derivatives of coenzyme A inhibit platelet function via antagonism at P2Y1 and P2Y12 receptors: a new finding that may influence the design of anti-thrombotic agents. *Platelets* **19**, 134-145 (2008).
42. Skrede, S. & Halvorsen, O. Mitochondrial biosynthesis of coenzyme A. *Biochemical and biophysical research communications* **91**, 1536-1542 (1979).
43. Rhee, H.W. *et al.* Proteomic mapping of mitochondria in living cells via spatially restricted enzymatic tagging. *Science* **339**, 1328-1331 (2013).
44. Leonardi, R., Rock, C.O., Jackowski, S. & Zhang, Y.M. Activation of human mitochondrial pantothenate kinase 2 by palmitoylcarnitine. *Proceedings of the National Academy of Sciences of the United States of America* **104**, 1494-1499 (2007).
45. Fiermonte, G., Paradies, E., Todisco, S., Marobbio, C.M. & Palmieri, F. A novel member of solute carrier family 25 (SLC25A42) is a transporter of coenzyme A and adenosine 3',5'-diphosphate in human mitochondria. *The Journal of biological chemistry* **284**, 18152-18159 (2009).
46. Moolman, W.J., de Villiers, M. & Strauss, E. Recent advances in targeting coenzyme A biosynthesis and utilization for antimicrobial drug development. *Biochemical Society transactions* **42**, 1080-1086 (2014).
47. Saliba, K.J. & Spry, C. Exploiting the coenzyme A biosynthesis pathway for the identification of new antimalarial agents: the case for pantothenamides. *Biochemical Society transactions* **42**, 1087-1093 (2014).
48. Mandel, A.L., La Clair, J.J. & Burkart, M.D. Modular synthesis of pantetheine and phosphopantetheine. *Organic letters* **6**, 4801-4803 (2004).

SUPPLEMENTARY METHODS

Drosophila S2 Cell Culture, RNA Interference, and CoA and 4'-phosphopantetheine treatment

Drosophila Schneider's S2 cells were maintained at 25°C in Schneider's *Drosophila* medium (Invitrogen) supplemented with 10% fetal calf serum (Gibco) and antibiotics (penicillin/streptomycin, Invitrogen) under laboratory conditions. Synthesis of RNAi constructs and RNA interference (dsRNA) treatment was carried out as described previously[4]. Non-relevant (human gene; hMAZ) dsRNA was used as control. The cells were incubated for 4 days to induce an efficient knock-down. Cells were then subcultured, with or without CoA (Sigma-Aldrich, Cat. No: C4780, 95% – which is used for all the experiments wherever stated below) or 4'-phosphopantetheine (PPanSH) (Acies Bio, >92%) at different concentrations and were maintained for additional 3 days until analysis for rescue efficiency of the compounds was performed. The stock solutions of compounds were made in sterile water and stored in -20°C until use.

HoPan treatment of *Drosophila* S2 Cell in combination with CoA or 4'-phosphopantetheine treatment

Drosophila Schneider's S2 cells were maintained at standard conditions as explained above. Cells in the exponential phase of growth were used for all the experiments. Different indicated concentrations of CoA or 4'-phosphopantetheine (deuterium labelled PPanSH(D4) or unlabelled PPanSH) were added to S2 cells either in the presence or absence of 0.5mM HoPan (Zhou Fang Pharm Chemical,; 99%) for 48hrs. Similarly, *Drosophila* S2 cells were treated with different concentrations of PPanSH(D4) at either 25°C or 4°C and cells were then harvested at various time points to access transport of PPanSH(D4). Stable isotope labelled PPanSH containing 4 deuterium atoms was purchased as a sodium salt (from Syncom; synthesized as previously described[48], 99.7%). As a read out, cell count, intracellular total CoA and PPanSH levels (both labelled and unlabeled levels wherever appropriate) and histone acetylation levels were analyzed as explained below.

Drosophila S2 Cell Immunofluorescence Staining

For immunofluorescence *Drosophila* S2 cells were seeded on Poly-L-Lysine coated (Sigma-Aldrich) glass microscope slides and allowed to settle for 45min. Cells were fixed with 3.7% formaldehyde (Sigma Aldrich) for 20min, washed briefly with phosphate-buffered saline (PBS) + 0.1% Triton-X-100 (Sigma Aldrich) and permeabilized with PBS + 0.2% Triton-X-100 for 20min. The slides were incubated in primary antibody (rabbit anti-AcLys, Cell Signaling Cat No: 9441, 1:500) to visualize histone acetylation levels in PBS + 0.1% Triton-X-100 overnight and after an additional washing step in PBS + 0.1% Triton-X-100 they were incubated in secondary goat anti-rabbit-Alexa488 antibody (Molecular Probes) for two hours at room temperature (RT). F-actin was detected with Rhodamin-Phalloidin (20U/ml) (Invitrogen) and DNA by staining with DAPI (0.2_g/ml) (Thermo Scientific). Finally the samples were mounted in 80% glycerol and analyzed using a Leica fluorescence microscope with Leica software. Adobe Photoshop and Illustrator (Adobe Systems

Incorporated, San Jose, California, USA) were used for image assembly.

HoPan treatment of mammalian HEK293 Cells in combination with CoA and 4'-phosphopantetheine treatment

HEK293 cells were maintained in dMEM (Invitrogen) supplemented with 10% fetal calf serum (Gibco) and antibiotics (penicillin/streptomycin, Invitrogen). For HoPan treatment, cells were cultured in custom made dMEM without Vitamin B5 (Thermo Scientific) supplemented with dialyzed FCS (Thermo Scientific). CoA or PPanSH was added to HEK293 cells for the final concentration of 25μM, either in the presence or absence of HoPan (0.5mM) for 4 days, followed by analysis for phenotype and rescue efficiency of CoA and PPanSH.

Knockdown of COASY by siRNA in mammalian HEK293 cells

HEK293 cells were maintained as described above. HEK293 cells were transfected with 200nM COASY siRNA (GE Healthcare human COASY 80347 smartpool Cat no: M-006751-00-0010) or non-targeting siRNA (GE Healthcare Cat no: D-001206-13-20) using lipofectamine 2000 (Invitrogen). 4hrs after transfection CoA was added in a final concentration of 25μM. Cells were cultured for 3 days and then harvested for HPLC analysis of total CoA and PPanSH levels and Western blot (histone acetylation) as described below.

Western blot analysis and Antibodies

For Western blot analysis, cells were collected and washed with PBS, followed by centrifugation. The cells were lysed and sonicated in 1X Laemmli Sample Buffer and boiled for 5min with 5% β-mercaptoethanol (Sigma). Protein content was determined using DC protein assay (BioRad). Equal amounts of protein were loaded on a 10 or 12.5% SDS-PAGE gel, transferred onto PVDF membranes and blocked with 5% milk in PBS/0.1% Tween, followed by overnight incubation with primary antibodies. The primary antibodies used were: rabbit-anti dPANK/fbl, 1:4000 Eurogentec custom made as described previously[12], mouse anti-tubulin (Sigma Aldrich Cat no: T5168, 1:5000), anti-acetyl-Histone3 (Active Motif Cat no: 39139, 1:2000), anti GAPDH (Fitzgerald Cat no: 10R-G109a, 1:10000), rabbit anti COASY (Abcam Cat no: AB129012, 1:1000). Appropriate HRP-conjugated secondary antibodies (Amersham) were used and detection was performed using enhanced chemi-luminescence (Pierce cat nog: 32106) and Amersham hyperfilm (GE healthcare). Band intensities were quantified with Image-studio software. Full uncut gel images for all Westerns displayed in this paper are shown in Supplementary Figures 15 and 16.

C. elegans Media and Strains:

Standard culturing conditions were used for *C. elegans* maintenance at 20°C. N2 strain was used as a wild-type control. VC927, the PANK deletion mutant *pnk-1 (ok1435)I/hT2[bli-4(e937) let-? (q782)qIs48] (I;III)*, was obtained from the *Caenorhabditis* Genetics Center. To obtain synchronous cultures, worms were bleached with hypochlorite, and allowed to hatch in M9 buffer (3g KH_2PO_4, 6g Na_2HPO_4, 5g NaCl, 1ml

1M $MgSO_{4'}$ H_2O to 1 liter) overnight and cultured on standard Nematode Growth Medium (NGM) plates seeded with OP50 strain of *Escherichia coli*.

C. elegans lifespan assay

After synchronization, *C. elegans* L1 animals were grown on control NMG plates or NGM plates supplemented with 400μM CoA. The life span experiments were started by transferring 100 one-day old adults per condition on NGM plates, which contained 5-fluoro-2′deoxy-uridine (FUDR) to inhibit growth of offspring. Once a day surviving animals were counted, the worms that disappeared or crawled out of the plate were excluded from the analysis.

C. elegans motility assay

After synchronization, L1 *C. elegans* were grown on control NMG plates or NGM plates containing various concentrations of CoA. One-day old adults were placed in a drop of M9 buffer and allowed to recover for 30sec. During the following 30sec, the number of body bends were counted. A movement was scored as a bend when both the anterior and posterior ends of the animal turned to the same side. At least 15 worms were scored per condition and each experiment was repeated thrice. The sequential light microscopy images demonstrating movements of *C. elegans* in M9 buffer were captured using Leica MZ16 FA microscope at 32x magnification within the time frame of 1sec and processed using ImageJ (National Institutes of Health, Maryland, USA) and Adobe Photoshop (Adobe Systems Incorporated, San Jose, California, USA).

Drosophila maintenance and crosses

Drosophila melanogaster stocks/crosses were raised on standard cornmeal agar fly food (containing water, agar 17 g/L, sugar 54 g/L, yeast extract 26 g/L and nipagin 1.3 g/L) at 25°C. The stocks were either obtained from the Bloomington Stock Centre (Indiana University, USA), VDRC (Vienna *Drosophila* RNAi Collection, Vienna, Austria) or from the Exelixis Collection (Harvard Medical School) and rebalanced over eGFP-positive balancers to identify homozygous (eGFP negative) progeny. The stocks used were: *w[1118]; dPANK/fbl*^{1} hypomorph[12,19]; *dPANK/fbl*^{null} (y[1] w[*]; *Mi{y[+mDint2]=MIC}fbl[MI04001]/TM3, Sb[1] Ser[1],* Bloomington 36941); *dPPCDC* mutant *(w[1118]; PBac{w[+mC]=WH}Ppcdc[f00839]/CyO*, Bloomington 18377); UAS-*dPPCDC* RNAi line (VDRC 104495); *dCOASY* mutant *(PBac{RB}Ppat-Dpck[e00492]*, Exelixis). The UAS-RNAi constructs were expressed ubiquitously using the *Actin-Gal4* drivers (*y[1] w[*]; P{w[+mC]=Act5C-GAL4}25FO1/CyO, y[+]*, Bloomington 4414). As controls we used the heterozygous flies/larvae for the mutants and the Actin-Gal4 driver crossed to isogenic *w1118* flies (*Actin-Gal4/+*) for the RNAi-constructs expressing flies.

Drosophila larval collection and larval count experiment

One week old flies (in the ratio 10 females and 5 males) were kept on 5ml of standard fly food in a vial at 25°C with or without various concentrations of CoA or Vitamin B5 (Sigma, Cat. No. P5155). The flies were

allowed to lay eggs for 2 days and parent flies were then discarded. The L1, L2 and L3 larvae were collected from the food with 20% sucrose at appropriate time (day 4, 6 and 8 respectively) for larval counting and stored in -80°C until analysis. The pupal count was performed between 10-12 days.

Drosophila HoPan Toxicity and CoA Rescue Experiment

One week old *w1118* flies (in the ratio 10 females and 5 males) were kept in vials containing standard fly food with or without HoPan and CoA at indicated concentrations. The flies were allowed to lay eggs for 2 days, after which the adults were discarded. The resulting offspring were allowed to develop. The numbers of flies which eclosed were counted to evaluate HoPan toxicity and CoA rescue efficiency.

Drosophila life span

One-day old female adult flies of *Drosophila* homozygous mutants or RNAi-constructs expressing lines, were collected with appropriate controls and were kept on standard fly food at 25°C with or without CoA or Vitamin B5 (Sigma) at necessary concentration (in 50µl added on top of the fly food and dried before flies were added). The flies were counted every 12-24hrs and flipped to new fly food vials with or without CoA or Vitamin B5.

Drosophila ovary rescue experiment

UAS-dPPCDC RNAi constructs were ubiquitously expressed under the control of *Actin-Gal4*. The crosses were raised at 25°C. F1 RNAi-construct expressing females and control females were collected shortly after eclosion and transferred to standard fly food or food containing Vitamin B5 or CoA (18mM). Flies were maintained for 2 days on this food at 25°C. After this period extra yeast and *w1118* control males were added and the crosses were kept at 25°C for another 2 days. After this 4 day period ovaries were dissected and stained for further analysis. The vials (or plates) from the crosses (with eggs that were being laid during the 4 day period of CoA treatment) were kept for another 10 days and offspring numbers were counted after eclosion.

RNA isolation, quantitative Real-Time PCR, and primers

Drosophila larvae and samples of 1-day old adult flies or larvae were collected for homozygous *dPPCDC* mutants, *dPPCDC* RNAi-construct expressing lines and for homozygous *dCOASY* mutants, followed by brief washing with PBS. The samples were lysed in TRIZOL (Invitrogen) for RNA extraction and reverse transcribed using M-MLV (Invitrogen) and oligo(dt) 12-18 (Invitrogen). SYBR green (Bio-Rad) and Bio-Rad Real-Time PCR with specific primers were used for gene expression level analysis. The expression levels were normalized for rp49 (house-keeping gene). The Primer sequences used were *dPPCDC* (TGCACCTGCGATGAATACCC; TCGGCTGAAAGGCGGATAAC), *dCOASY* (GGCTGTGCGGCGGATTATTG; CGGGTTAAAGGCTGCTCTGG) and *rp49* (GCACCAAGCACTTCATCC; CGATCTCGCCGCAGTAAA) (Biolegio).

Drosophila ovary dissection and staining

Drosophila ovaries were collected in cold PBS and fixed in 4% formaldehyde (from methanol-free 16% Formaldehyde Solution, Thermo Scientific) for 45min at RT. The fixed tissue was washed in PBS + 0.1% Triton-X-100 for 1hr at RT and afterwards permeabilized in PBS + 0.2% Triton-X-100 for 1hr. Finally the ovaries were stained with Rhodamin-Phalloidin (20U/ml) to detect F-actin and DAPI (0.2 _g/ml) for DNA. Finally the samples were mounted in 80% glycerol and analyzed on a Zeiss-LSM780 NLO confocal microscope with Zeiss Zen software. Adobe Photoshop and Illustrator (Adobe Systems Incorporated, San Jose, California, USA) were used for image assembly.

PAMPA assay procedure

Parallel Artificial Membrane Permeability Assay (PAMPA) was performed and processed according to manufacturer's instructions (BD Gentest Pre-coated PAMPA plates). Briefly, two superimposed wells are separated by an artificial lipid-oil-lipid membrane. The compound of interest (PPanSH, CoA, caffeine, amiloride) was added to the bottom well in phosphate-buffered saline, whereas the top well was filled with phosphate-buffered saline alone. After 5hrs of incubation at RT, concentrations of the different compounds were measured using UV-VIS absorption spectroscopy (BMG Labtech SPECTROstar Omega) along with calibration curves for all compounds. The permeability efficiency was further calculated according to manufacturer's instructions (Supplementary figure 9e). For caffeine and amiloride, four replicates were performed; for PPanSH and CoA twelve replicates were performed. Caffeine and amiloride were obtained from Sigma.

Serum collection from PKAN patients

Serum was collected from the blood of PKAN patients and respective healthy family members (control) using standard protocols. Briefly, venous blood was collected in commercially available red topped Vacutainer tubes (Becton Dickinson) and allowed to remain at RT for 15-30min undisturbed for the blood clotting. The tubes were then centrifuged at 2,000 g for 10min at 4°C. The resulting supernatant serum was immediately transferred to 2ml cryovials and maintained at -80°C until CoA stability assessments were performed. Blood samples and clinical data were obtained under OHSU's IRB-approved repository protocol #7232 following informed consent.

CoA and pantethine serum stability measurements

CoA serum stability studies were conducted in commercially obtained serum and in serum collected from PKAN patient and healthy family members as controls. Human and Mice sera were purchased from Sigma and Fetal calf serum was purchased from Gibco. Additionally, dMEM medium with or without 10% fetal calf serum was used for evaluating CoA stability. Briefly, all sera and samples were incubated for 30min at 37°C with or without pre-conditioning compounds at final concentration 10mM [Adenosine 5′-triphosphate (ATP), Adenosine 5′-diphosphate (ADP), Ethylenediaminetetraacetic acid (EDTA), Levamisole, Suramin, 4,4′-Diisothiocyanatostilbene-2,2′-disulfonic acid disodium (DIDS) and sodium fluoride (NaF), all

purchased from Sigma] followed by addition of CoA 20μM in the ratio of 1:1 and incubated at 37°C after brief vortex for indicated time intervals. For heat inactivation, all sera were incubated for 30min at 56°C after which CoA was added. Serum samples at different time points were collected, deproteinized and analyzed by HPLC as described below. For pantethine serum stability, pantethine (Sigma) was incubated in fetal calf serum, mice serum and human serum for 15min in 37°C and total levels of pantetheine and cysteamine was measured using HPLC.

Mice and CoA intravenous injection study

Adult male mice of C57BL/6J 129/SvJ mixed genetic background were used for this study. Two mice (approximately 25-30g wt) were used for each condition. 0.1mg or 0.5mg CoA in 0.25ml saline solution was injected intravenously (i.v) into the tail vein. Saline solution (0.25ml) was injected to control groups. After 30min and 6hrs blood samples were collected and further processed to obtain plasma followed by sample preparation for HPLC or LC-MS analysis as indicated below. All animal studies were approved by the Ethics Committee of the Foundation IRCCS Neurological Institute C. Besta, in accordance with guidelines of the Italian Ministry of Health: Project no. BT4/2014. The use and care of animals followed the Italian Law D.L. 116/1992 and the EU directive 2010/63/EU.

HPLC sample preparation protocol for total CoA and 4'-phosphopantetheine measurement

Samples were briefly washed with ice-cold PBS solution. Samples were sonicated thoroughly in 100μl ice-cold PBS and centrifuged for 10-15min at 4°C to collect supernatant. Tris(2-carboxyethyl)phosphine hydrochloride (Sigma) (50mM; 10μl) was added to 50μl sample supernatant and were incubated at RT for 15min after vortex-mixing. Saturated ammonium sulfate solution or Millipore 3KD centrifugal filter units were used to remove proteins. The samples were centrifuged at 14,000 rpm for 15min at 4°C. The clear supernatant (50μl) or the filtrate was derivatized with 45μl of ammonium 7-flurobenzo-2-oxa-1,3-doazole-4-sulfonate (SBD-F, Sigma) (1mg/ml in borax buffer - 0.1M containing 1mM EDTA disodium, pH 9.5), and 5μl ammonia solution (12.5% v/v, Merck Millipore) at 60°C for 1hr. The derivatized samples were placed in a refrigerated autosampler (10°C) in the Shimadzu HPLC system, and injected for total CoA and PPanSH analysis using optimized chromatographic separation conditions combined with fluorescence detection (described below).

Chromatography separation condition

Chromatographic analysis was performed with a Shimadzu LC-10AC liquid chromatograph, SCL-10A system controller, SIL-10AC automatic sample injector and LC-10AT solvent delivery system. Shimadzu RF-20Axs fluorescence detector was used for derivatized sample extract analysis. The fluorescence detector was set at excitation and emission wavelengths of 385nm and 515nm, respectively. Signal output was collected digitally with Shimadzu Labsolution software and postrun analysis were performed. Chromatographic separation of the analytes was achieved with a Phenomenex Gemini C18 guard column (4 x 3mm) connected to a Phenomenex Gemini NX-C18 analytical column (4.6 x 150mm; 3μm particles) at 45°C. The two mobile phases consisted of A: 100mM ammonium acetate buffer (pH 4.5) and B:

acetonitrile. Flow rate was maintained at 0.8ml/min with a slow gradient elution: 0% B till 7min, 20% B at 20min, 20% B at 22min, 50% B at 23min, maintained at 50% B till 27min, 0% B at 28min and 7-10min for column re-equilibration.

Sample preparation for mass spectrometry and instrumental parameters

Samples were briefly washed with ice-cold PBS solution. Samples were then sonicated thoroughly in 100µl ice-cold milliQ (MQ) water containing 50mM Tris(2-carboxyethyl)phosphine hydrochloride. Subsequently 100µl saturated ammonium sulfate was added to each sample and centrifuged for 20 min at 10°C, 16,100 rcf to collect supernatant. To 150µl of supernatant, 15µl of ammonium hydroxide (12.5%) was added and 20µl was injected for LC-MS (liquid chromatography-mass spectrometry) analysis. For mouse plasma analysis, 50µl of MQ water containing 50mM Tris(2-carboxyethyl)phosphine hydrochloride was added to 50µl of plasma and processed further as mentioned above. Appropriate dilution series of standard CoA, PPanSH and PPanSH(D4) was processed similarly before analysis. The LC separation of metabolites were obtained using Phenomenex Gemini NX-C18 analytical column (4.6 x 150mm; 3µm particles) at 45°C. The flow was maintained at 1ml/min with optimized mobile phase gradient of MQ water (A), 200mM ammonium acetate (NH_4Ac) in 95/5 MQ water/acetonitrile adjusted to pH 4.5 with acetic acid (B), and acetonitrile (C). The separated analytes were detected with positive mode mass spectrometry (Sciex API5500 Q-trap) under unit resolution. The targeted Q1/Q3 mass/charge ions of PPanSH, PPanSH(D4), CoA and CoA(D4) were 359.1/261.1, 363.1/265.1, 768/261.1, and 772/265.1 respectively. The absolute concentration was finally calculated using linear regression analysis of respective standard compounds, except CoA(D4) which was estimated indirectly using CoA standards.

Statistical Analysis

All experimental results are presented as mean of at least 3 independent experiments ± SD, unless otherwise stated. Statistical significance was determined by a two-tailed unpaired Student's t test between appropriate groups wherever applicable. For life span survival curve, more than 80 flies or *C.elegans* were used in each group and statistical significance was determined using Log-rank (Mantel-Cox) test (See figure legends for exact number or flies/*C.elegans* used in survival analysis). Statistical P values ≤ 0.05 were considered significant (*P ≤ 0.05, **P ≤ 0.01, ***P ≤ 0.001). Data were analyzed using GraphPad Prism (GraphPad Software, San Diego, CA, USA).

SUPPLEMENTARY FIGURES

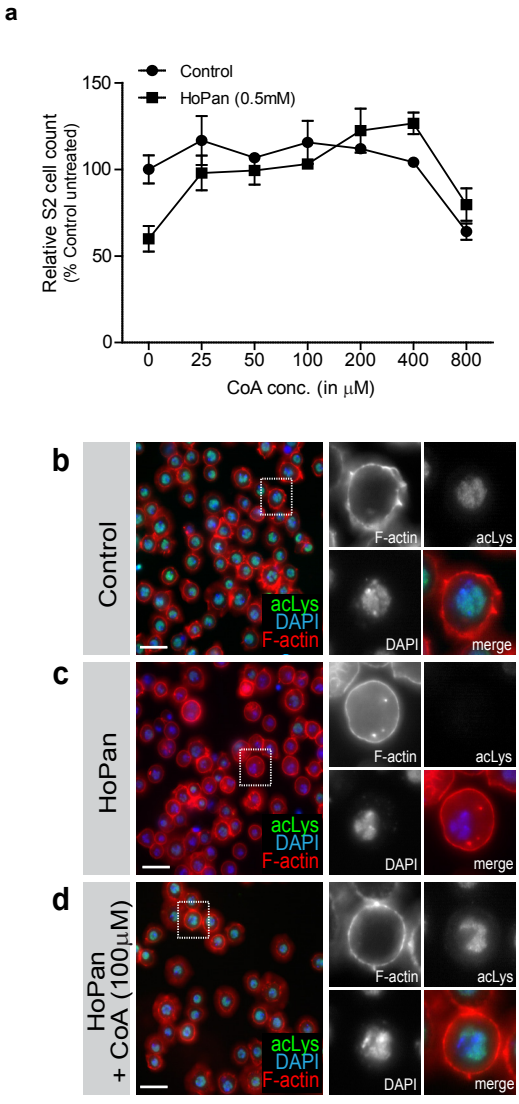

Supplementary Figure 1: CoA supplementation rescues HoPan induced phenotypes in *Drosophila* S2 cultured cells. **a.** Relative cell counts of control (100%) and HoPan treated cells in the presence of increasing concentrations of CoA. Data points represent mean ± SD (n = 3). **b-d**. Protein acetylation levels were visualized in control (**b**) and HoPan treated cells without (**c**) and with (**d**) CoA. An antibody against acetylated Lysine (green), Rhodamin-Phalloidin (red), marking F-actin, and DAPI (blue, DNA) were used. Scale bars indicate 20μm.

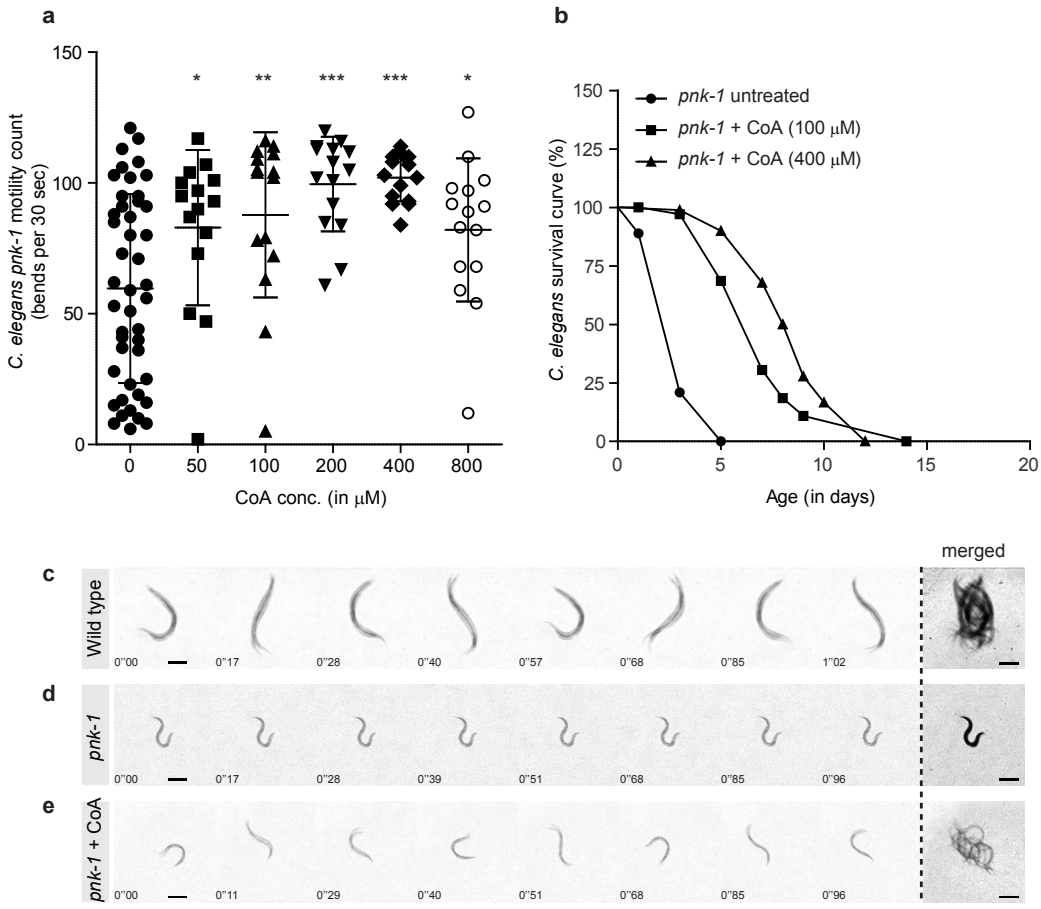

Supplementary Figure 2: Phenotypes induced by impaired pantothenate kinase in *C. elegans* are rescued by external supplementation of CoA. a. Quantification of motility in *C. elegans* pantothenate kinase (*pnk-1*) mutants with and without addition of different CoA concentrations (0, 50, 100, 200, 400 and 800μM) to the food. Error bars indicate ± SD (n = 15, except for 0μM where n = 45) and two-tailed unpaired Student's t-test was used to assess statistical significance ($^{*}P \leq 0.05$, $^{**}P \leq 0.01$, $^{***}P \leq 0.001$). **b**. Lifespan analysis of *C. elegans pnk-1* mutants untreated (n = 96) and with CoA treatment (100μM; n = 101 and 400μM; n = 90). Survival curves were found to be significant with P value < 0.001, analyzed with Log-rank (Mantel-Cox) test, between untreated and CoA treated *pnk-1* mutants. **c-e**. Representative serial images demonstrating movements of *C. elegans* wild-type (**c**) and *pnk-1* mutants without (**d**) and with (**e**) CoA treatment (400μM); still images are given; "merged" indicates superimposed images. Scale bar represents 200μm.

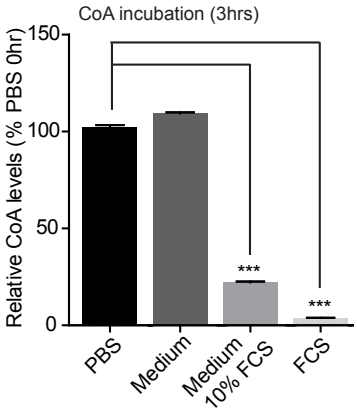

Supplementary Figure 3: CoA degradation profile in medium and fetal calf serum. Relative CoA levels determined by HPLC analysis in PBS, medium, medium containing fetal calf serum and in fetal calf serum (FCS) after 3 hrs incubation. Each bar represents mean data value (n = 3) ± SD and two-tailed unpaired Student's t-test was used to analyse significance ($^{***}P \leq 0.001$).

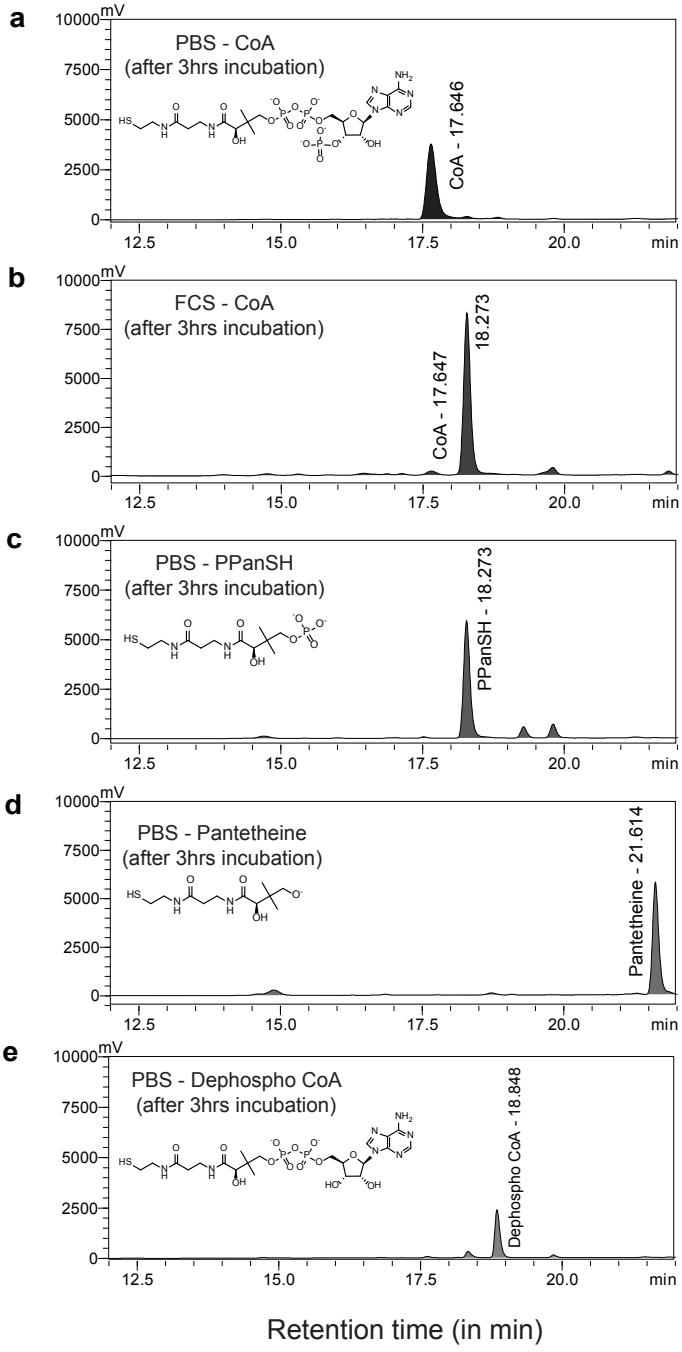

Supplementary Figure 4: Chromatogram profile of CoA and its thiol containing conversion product in fetal calf serum. a-e. HPLC chromatogram profile of CoA stability in PBS **(a)** and FCS **(b)** compared with standard 4'-phosphopantetheine (PPanSH, **c**), Pantetheine **(d)** and Dephospho-CoA **(e)**. CoA is migrating at 17.65 min; PPanSH at 18.27 min; Pantetheine at 21.61 min and Dephospho-CoA at 18.85. CoA is stable in PBS and converted in serum into a thiol-containing compound exactly migrating as PPanSH standard at 18.27 min.

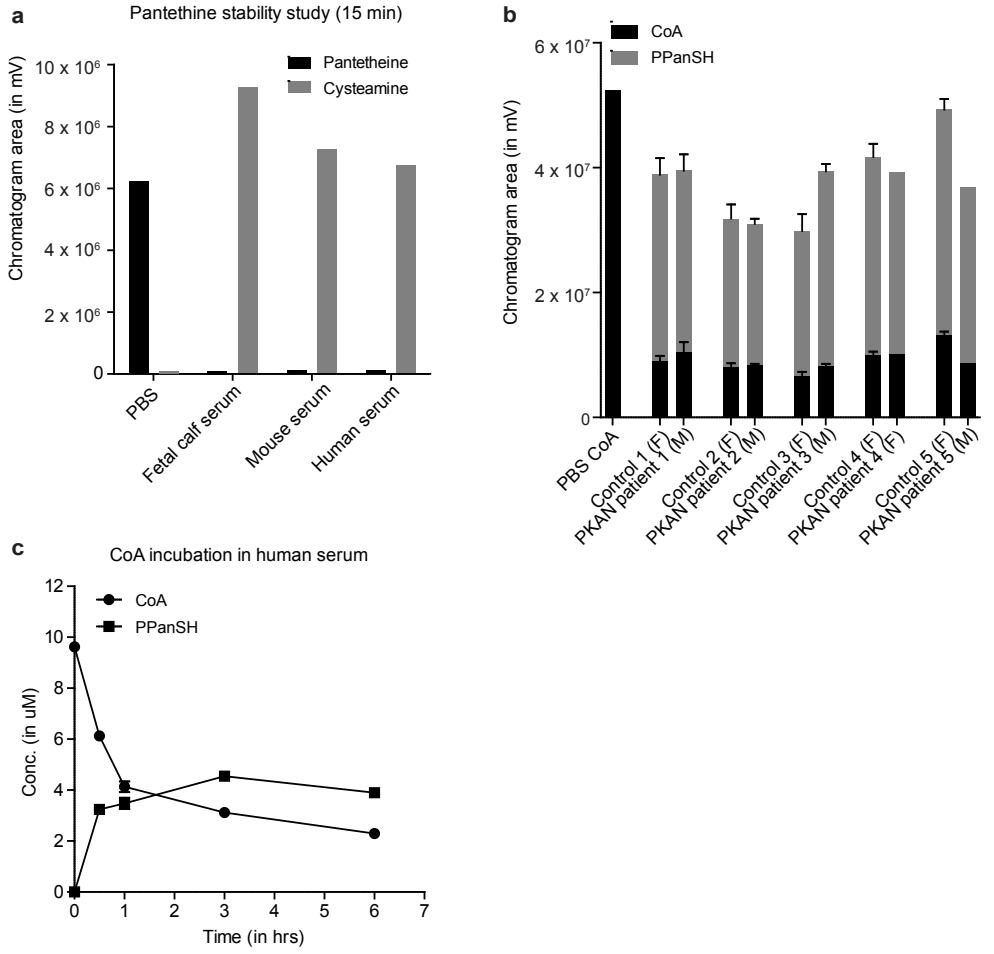

Supplementary Figure 5: Pantetheine stability, CoA conversion in patient's serum and CoA and 4'-phosphopantetheine stability in human serum. a. Pantethine is rapidly degraded in serum. Pantethine was incubated for 15min at 37°C in fetal calf serum, mice serum and human serum and levels of total pantetheine and cysteamine were measured using HPLC. **b**. CoA hydrolysis to PPanSH in serum derived from PKAN patients and their healthy family members as a control. CoA (20μM) was incubated for 3 hrs at 37°C in serum derived from PKAN patient and in serum derived from their healthy family members as a control. Levels of CoA and PPanSH were measured using HPLC analysis. In patient's serum CoA was as efficiently hydrolysed into PPanSH as in serum derived from healthy family members. Error bars represent ± SD where applicable for mean values (n = 3). Genders were indicated as female=F and male=M. **c**. CoA was added to human serum and concentrations of CoA and PPanSH in human serum over 6 hrs were determined by HPLC analysis. Data points indicate mean value ± SD (n = 3).

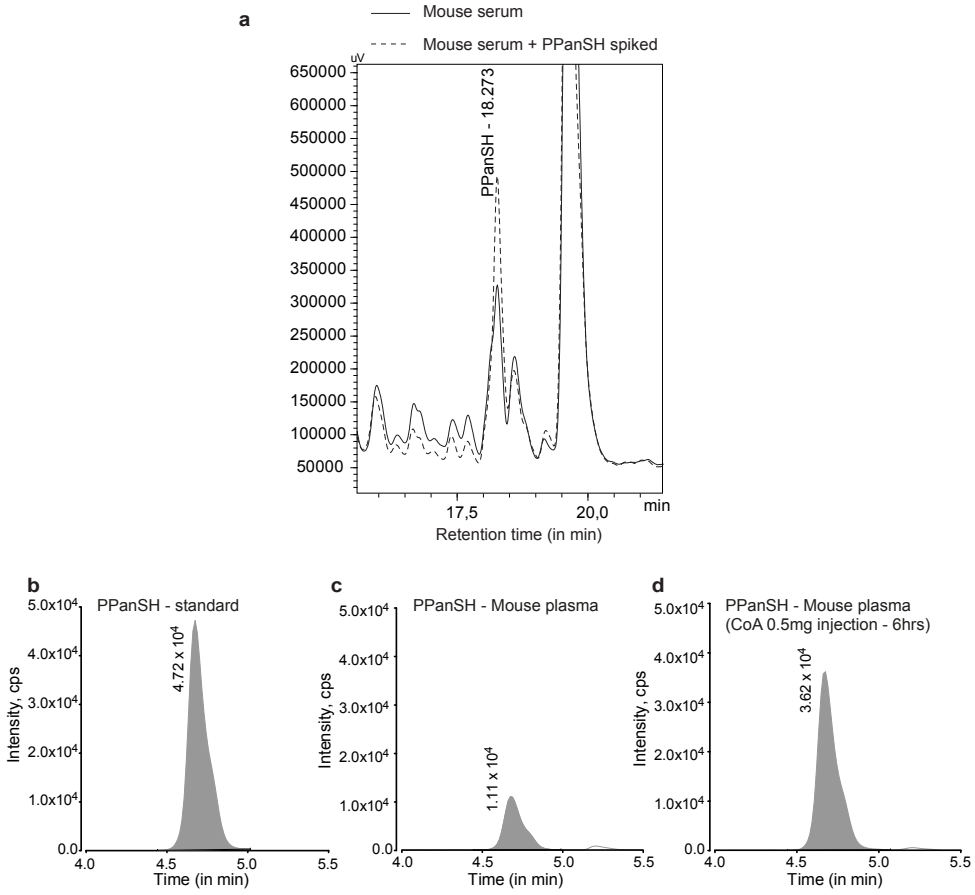

Supplementary Figure 6: HPLC chromatogram profile and confirmation by mass spectrometry of endogenous 4'-phosphopantetheine in mouse serum. a. HPLC chromatogram profile in untreated fresh mouse serum (solid line), shows a peak which co-migrates exactly with PPanSH as visible when the sample was spiked with standard PPanSH (dotted line). These results indicate the presence of endogenous PPanSH. **b-c**. Confirmation of endogenous PPanSH by mass spectrometry in mouse plasma (**c**) compared to standard PPanSH (**b**). **d.** Mass spectrometry was used to confirm the presence of elevated levels of PPanSH in plasma, 6 hrs after CoA injection (0.5mg) in mice.

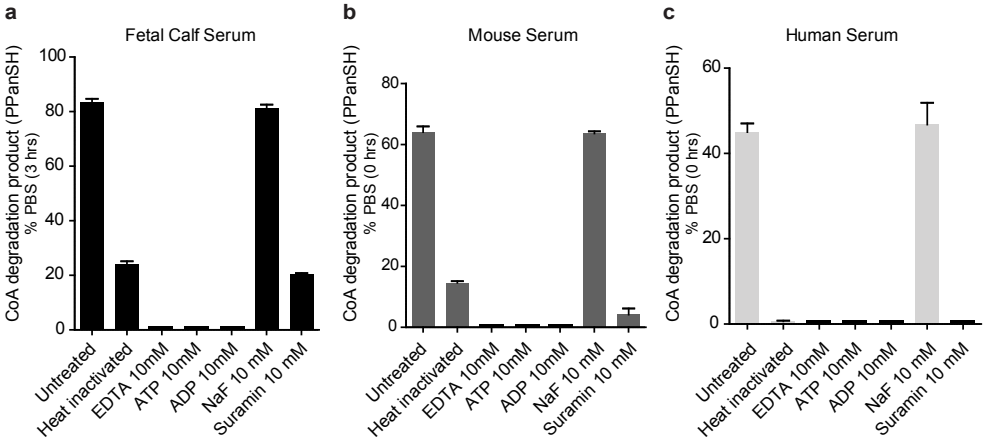

Supplementary Figure 7: CoA degradation correlates with the appearance of 4'-phosphopantetheine. **a-c**. 4'-phosphopantetheine measurements of the experiment shown in main Figure 4. Fetal calf serum (**a**), mouse serum (**b**) and human serum (**c**) were heat-inactivated or pre-treated with 10mM of EDTA, or ATP or ADP, or with the inhibitors Sodium fluoride (NaF) or Suramin and levels of PPanSH were determined as described for main Figure 4. Data represents mean value ± SD (n = 3) and solid black bars without error bars indicate no PPanSH was detected, wherever applicable.

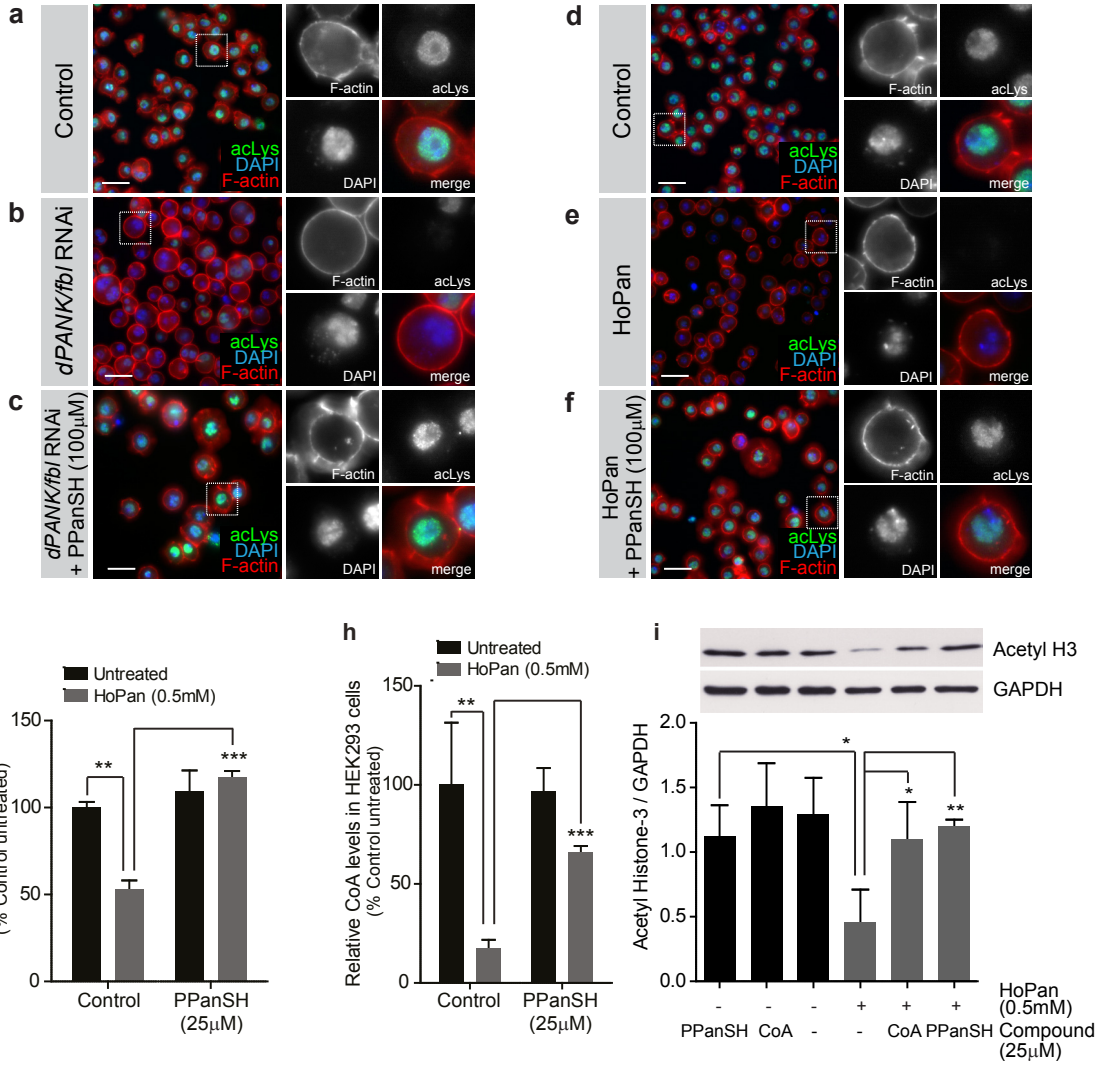

Supplementary Figure 8: External supplementation of 4'-phosphopantetheine rescues CoA-deprived phenotypes. a-f. Immunofluorescence was used to visualize protein acetylation levels in control (**a**,**d**), *dPANK/fbl* RNAi treated (**b**) and HoPan treated (**e**) S2 cells with and without PPanSH (**c**,**f**). An antibody against acetylated Lysine (green), Rhodamin-Phalloidin (red), marking F-actin, and DAPI (blue, DNA) were used. Addition of PPanSH rescues acetylation defects of *dPANK/fbl* RNAi and HoPan treated S2 cells. Scale bars indicate 20μm. **g**. Cell count of mammalian HEK293 control cells (100%), cells treated with HoPan with and without CoA or PPanSH added to the medium. Data indicate mean values ± SD (n = 3) and two-tailed unpaired Students t-test was used for statistical analysis. **h**. Relative CoA levels were determined by HPLC of control (100%) and HoPan treated HEK293 cells with and without CoA or PPanSH added to the medium. Data indicate mean values ± SD (n = 3) and two-tailed unpaired Students t-test was used for statistical analysis. **i**. Western blot analysis and quantification to determine histone acetylation levels of control HEK293 cells, cells treated with HoPan with and without CoA or PPanSH. Data represents mean values ± SD (n = 3) and two-tailed unpaired Students t-test was used for statistical analysis.

In all the above data representation, statistical significance was indicated as applicable ($^{*}P \leq 0.05$, $^{**}P \leq 0.01$, $^{***}P \leq 0.001$).

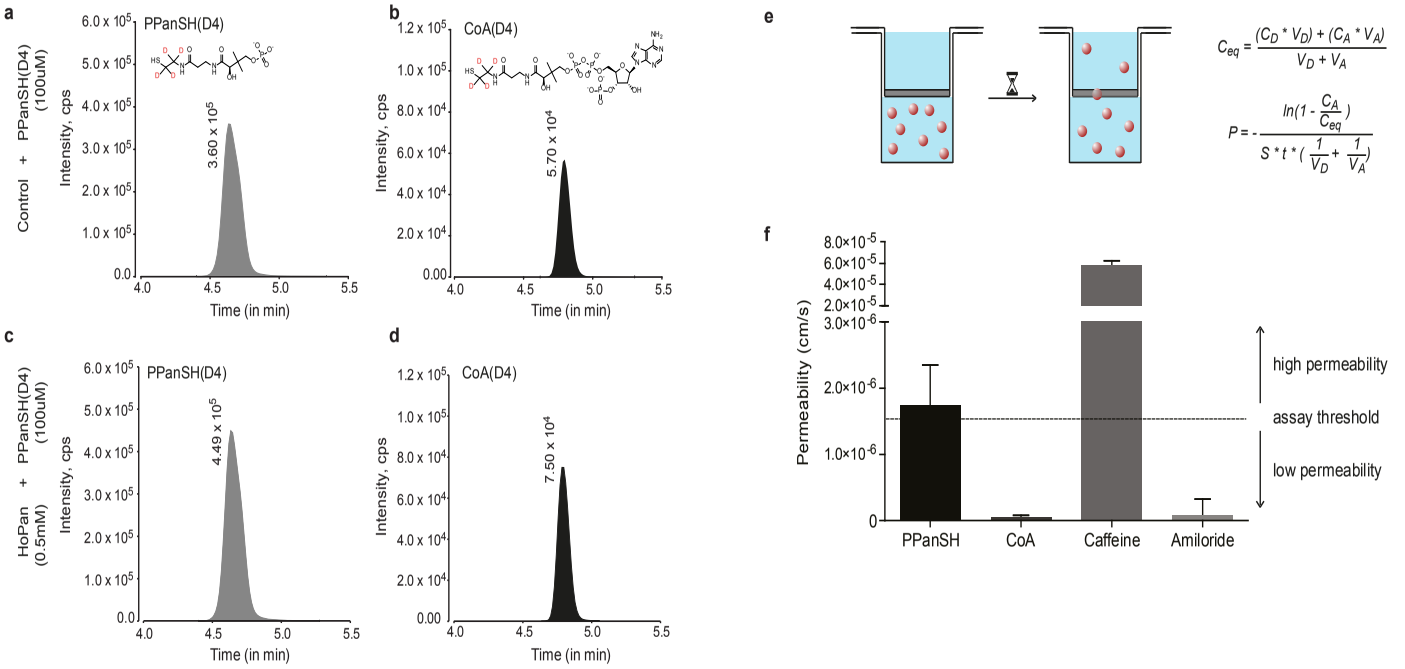

Supplementary Figure 9: 4'-phosphopantetheine is taken up by *Drosophila* S2 cells and converted in CoA. a-d. Mass spectrometry was used to detect the levels of 4'phosphopantetheine labelled with stable isotope (deuterium), PPanSH(D4) and CoA labelled with stable isotope (deuterium) (CoA(D4)). S2 cells were left untreated (**a**,**b**) or treated with HoPan (**c**,**d**) and PPanSH(D4) was added to the medium of untreated and HoPan treated cells. Levels of PPanSH(D4) (**a**,**c**) and levels of CoA(D4) (**b**,**d**) were measured. Chemical structures of PPanSH(D4) and CoA(D4) are given. **e-f.** Schematic overview of a Parallel Artificial Membrane Permeability Assay (PAMPA assay). Experiments were performed and the permeability parameter was calculated according to the manufacturer's instructions. (formulas are depicted in the figure and the parameters are explained below). (**f**) Compounds that are below the assay threshold are predicted to be unable to pass membranes passively, whereas compounds above the threshold are able to pass membranes passively. In contrast to CoA, PPanSH shows a permeating property (although the permeability parameter of PPanSH is lower compared to the positive control). Caffeine and amiloride were used as a positive and negative control respectively. Data values represents mean ± S.E.M with replicated for PPanSH and CoA; n = 12 and caffeine and amiloride; n = 4).

Abbreviations are as follows:

Ceq = Equilibrium Concentration
CD = Concentration in donor well
VD = Volume of donor well (0.3 ml)
CA = Concentration in acceptor well
VA = Volume of acceptor well (0.2 ml)
P = Permeability
S = Membrane area (0.3cm^2)
t = Incubation time (18000 s)

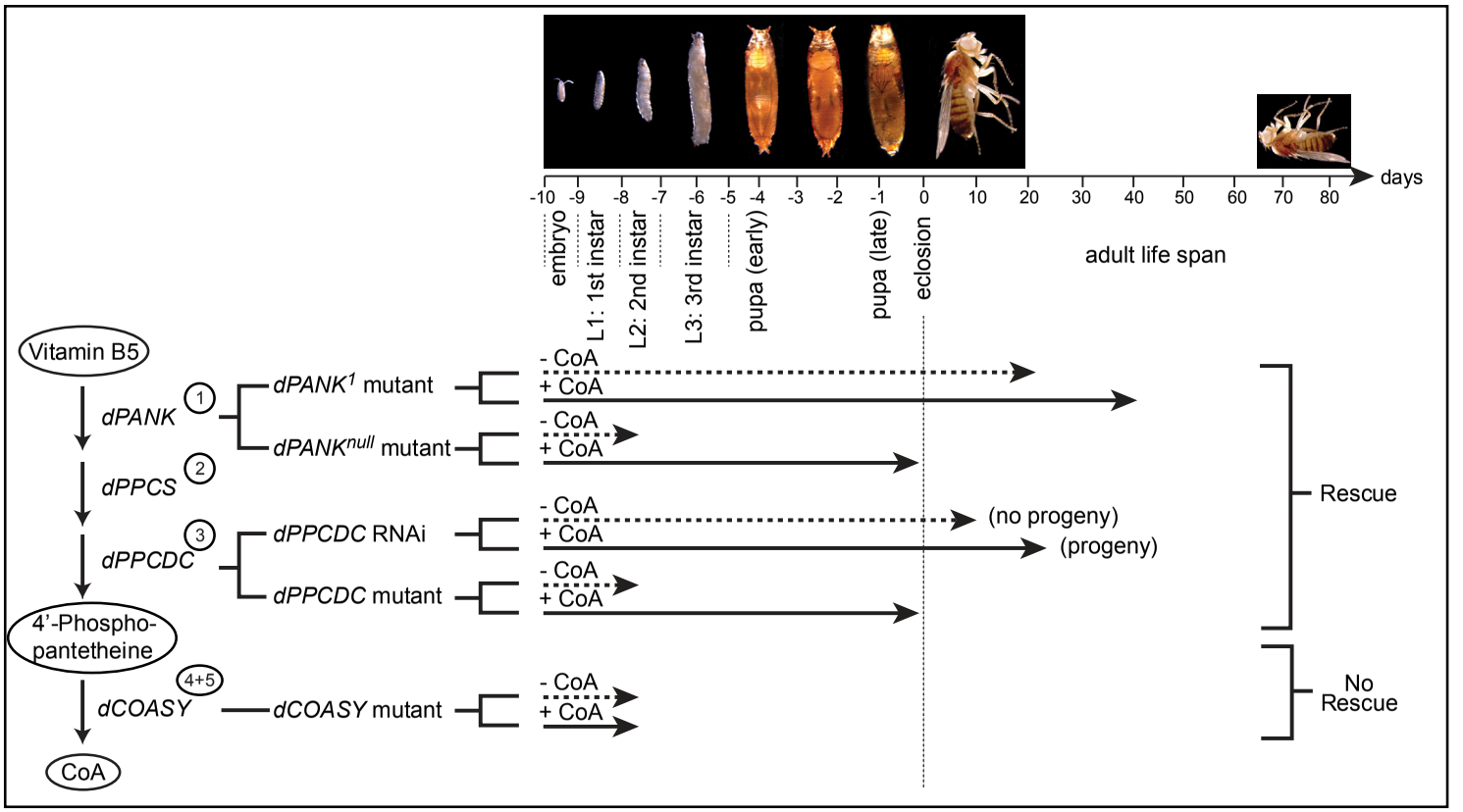

Supplementary Figure 10: External supplementation of CoA rescues *dPANK/fbl- and dPPCDC*- but not *COASY*-impaired phenotypes. From left to right; Overview of the well-known CoA biosynthesis route in which the enzymatic conversion steps 1, 2 and 3, upstream of PPanSH and the combined enzymatic step 4-5 downstream of PPanSH are indicated. Mutant lines and/or RNAi lines used for manipulating conversion steps upstream and downstream of PPanSH are indicated. The upper image represents time scale and images of normal *Drosophila* developmental and adult stages. Fly line and mutant-specific developmental arrest is indicated under control conditions (dotted line) and after CoA supplementation to the food (solid line).

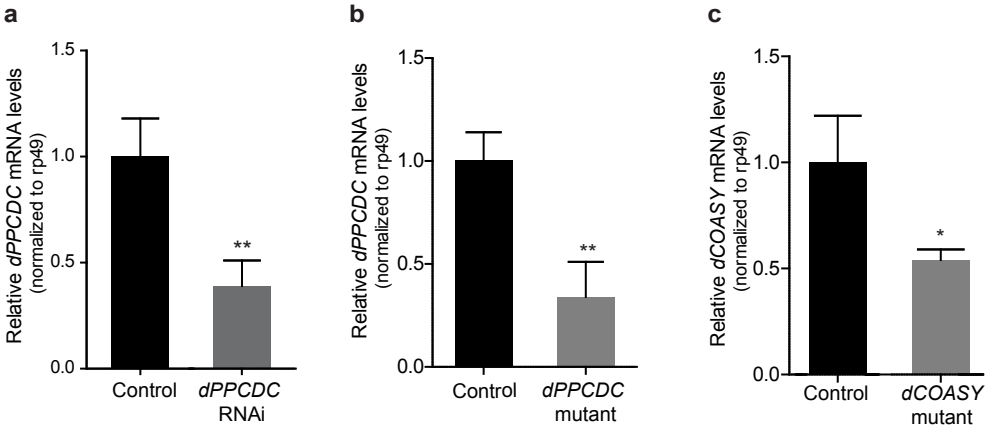

Supplementary Figure 11: Quantitative real-time PCR data demonstrates reduced mRNA expression of *dPPCDC* and *dCOASY* in *Drosophila* RNAi lines and mutant flies. a. mRNA expression levels of *dPPCDC* normalized with house-keeping gene (*rp49*) expression levels in 1-day old adult *dPPCDC* RNAi Drosophila female flies and in age-matched control flies. **b.** mRNA expression levels of *dPPCDC* normalized with house-keeping gene (*rp49*) expression levels in L2 stage control larvae and in L2 stage *dPPCDC* mutant larvae. **c.** mRNA expression levels of *dCOASY* normalized with house-keeping gene (*rp49*) expression levels in L1 stage control larvae and in L1 stage *dCOASY* mutant larvae.

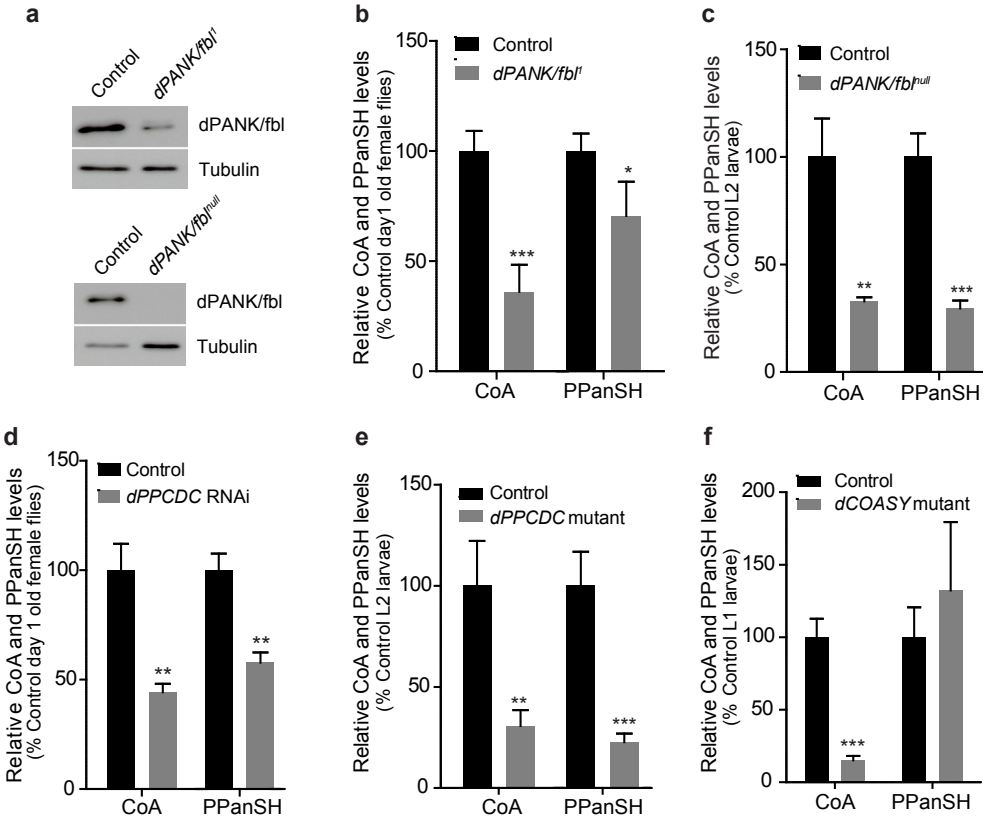

Supplementary Figure 12: External supplementation of CoA rescues *dPANK/fbl*- and *dPPCDC*- but not *COASY*-impaired phenotypes. a. Western blot analysis of dPANK/Fbl protein expression levels of control animals, homozygous hypomorphic (*dPANK/fbl*^{1}) mutants and homozygous null (*dPANK/fbl*^{null}) mutants. Tubulin as loading control. **b.** CoA and PPanSH levels measured by HPLC analysis in 1-day old hypomorphic homozygous (*dPANK/fbl*^{1}) mutant and control adult flies. CoA and PPanSH levels in mutant larvae are presented as percentages of CoA levels in control larvae. **c.** CoA and PPanSH levels measured by HPLC in early L2 stage null homozygous (*dPANK/fbl*^{null}) mutant and control larvae. CoA levels in mutant larvae are presented as percentages of CoA levels in control larvae. **d.** Relative CoA and PPanSH levels measured by HPLC in 1-day old females of the *dPPCDC* RNAi fly line compared to control flies. **e.** Relative CoA and PPanSH levels measured by HPLC of the L2 larval stage of control and homozygous *dPPCDC* mutant larvae. **f.** Relative CoA and PPanSH levels measured by HPLC of 1-day old homozygous *dCOASY* mutant larvae, compared to control. All the data sets in **b**-**f** indicate mean ± SD (n = 3) in the above representations and two-tailed unpaired Student's t-test was used for statistical analysis ($^{*}P \leq 0.05$, $^{**}P \leq 0.01$, $^{***}P \leq 0.001$).

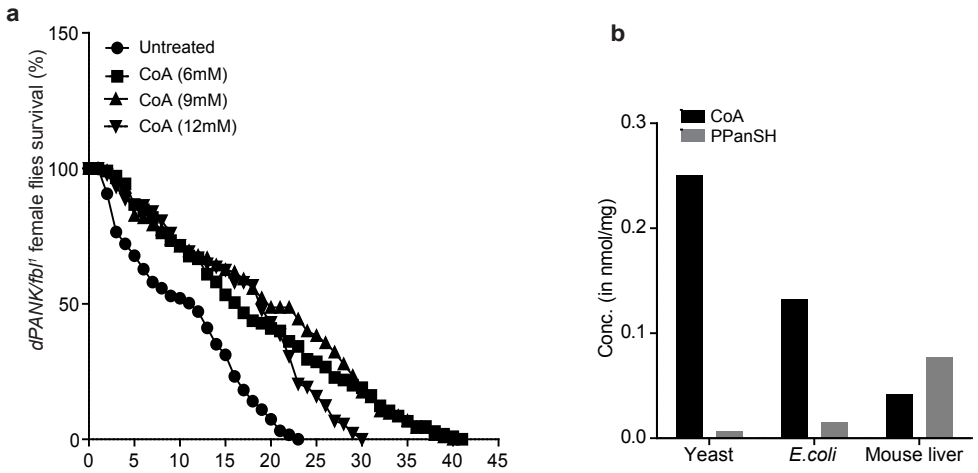

Supplementary Figure 13: Life span survival of *Drosophila dPANK* mutant flies and endogenous 4'-phosphopantetheine levels in food sources. a. Lifespan analysis of hypomorphic (*dPANK/fbl'*) homozygous female mutants untreated (n = 207) and treated with various concentrations of CoA (6mM, n= 105; 9mM, n = 115; and 12mM, n = 88) added to the food. Survival curves were found to be significant with P value < 0.001, analyzed with Log-rank (Mantel-Cox) test, between untreated and all CoA treated *dPANK/fbl'* mutants. **b**. In various animal food sources (yeast, E.coli and mouse liver) levels of CoA and PPanSH were measured and found to be present (n = 2).

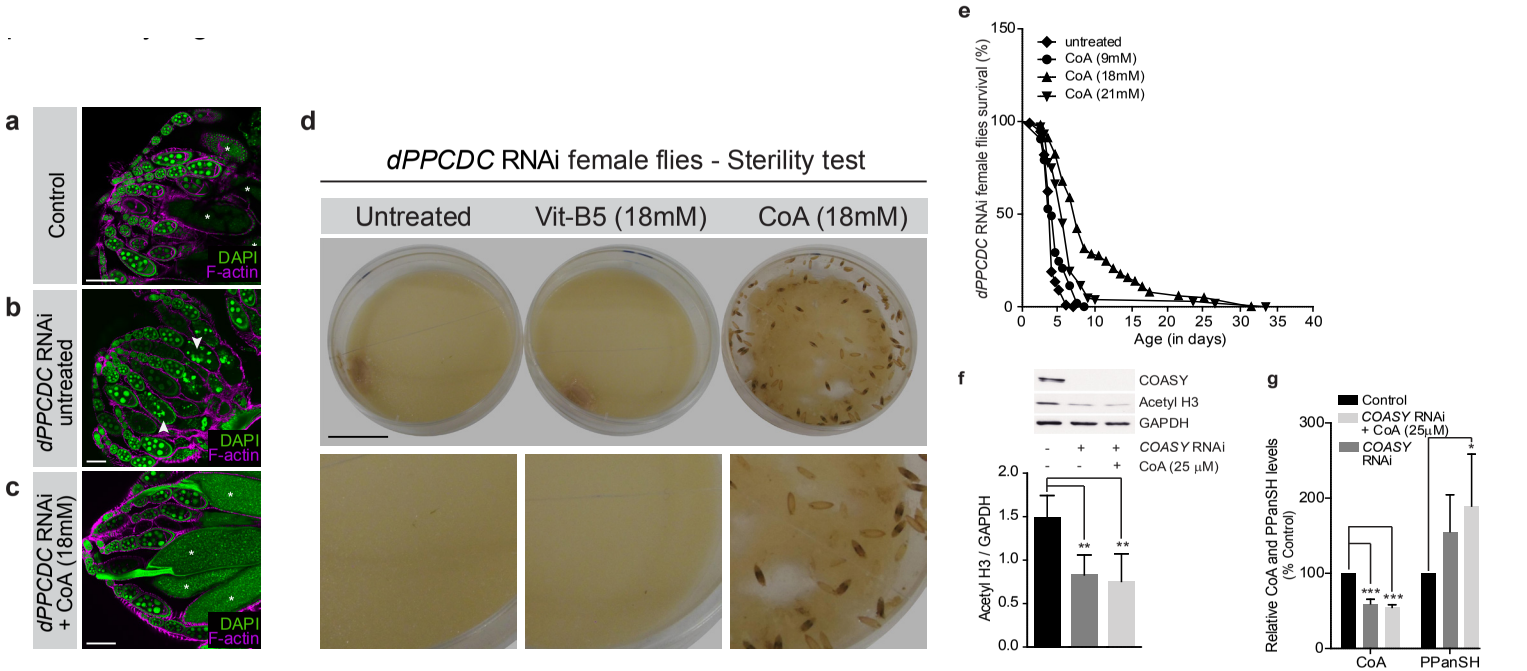

Supplementary Figure 14: External supplementation of CoA rescues phenotypes of dPPCDC RNAi lines and COASY is required for CoA rescue in mammalian cells. a-c. Ovaries of 4-day old control and *dPPCDC* RNAi expressing flies, stained with Rhodamin-Phalloidin (magenta, marking F-actin) and the nuclear marker DAPI (green) and imaged with confocal microscopy. (**a**) In wild-type ovarioles strings of developing egg-chambers, from the germarium up to stage 9 were visible. Mature eggs were also found (marked by asterisks), identifiable by the presence of yolk. (**b**) In ovaries of the *dPPCDC* RNAi expressing flies, egg-chambers developed normally until stage 7. From stage 8 on, fragmented and condensed DNA was visible, indicating apoptosis (marked by white arrowheads). No egg-chambers older than stage 8/9 or mature eggs were found in these ovaries. (**c**) CoA treatment of the *dPPCDC* RNAi expressing flies improved egg-production significantly and eggs developed to maturity (marked by asterisks). Scale bars =100μM. **d**. Increased fertility of *dPPCDC* RNAi expressing females. Untreated, Vitamin B5 treated and CoA treated *dPPCDC* RNAi expressing females were mated with control males and put onto apple juice plates to allow egg laying for 4 days. For untreated and Vitamin B5 treated females, no or only very few eggs were observed on the plates (compare Figure **6e**). CoA treated females produced a significant number of eggs that developed into pupae which eclosed resulting in viable offspring (compare Figure **6f**). Scale bar = 1 cm. **e**. Lifespan analysis of adult female *dPPCDC* RNAi flies untreated (n = 111) and treated with various concentrations of CoA (9mM, n = 106; 18mM, n = 102; 21mM, n = 104) added to the food. Survival curves were found to be significant with P value < 0.01 for CoA 9mM treatment and P value < 0.001 for CoA (18 and 21mM) treatment compared to control untreated *dPPCDC* RNAi *mutants*, analyzed with Log-rank (Mantel-Cox) test. **f.** RNAi was used to down-regulate *COASY* in HEK293 cells treated or non-treated with CoA and acetyl histone3 levels were quantified (n = 5). Insert: Western blot analysis showing successful down-regulation of human *COASY* by RNAi and decreased histone acetylation (and quantification). GAPDH was used as loading control. **g**. Relative levels of CoA and PPanSH were measured in control HEK293and *COASY* down-regulated cells treated with medium with and without addition of CoA (n = 4). The data (**f**,**g**) indicate the mean ± SD and two-tailed unpaired Student's t-test was used for statistical analysis ($^{**}P \leq 0.01$, $^{***}P \leq 0.001$).

Original blots used for Figure 1b

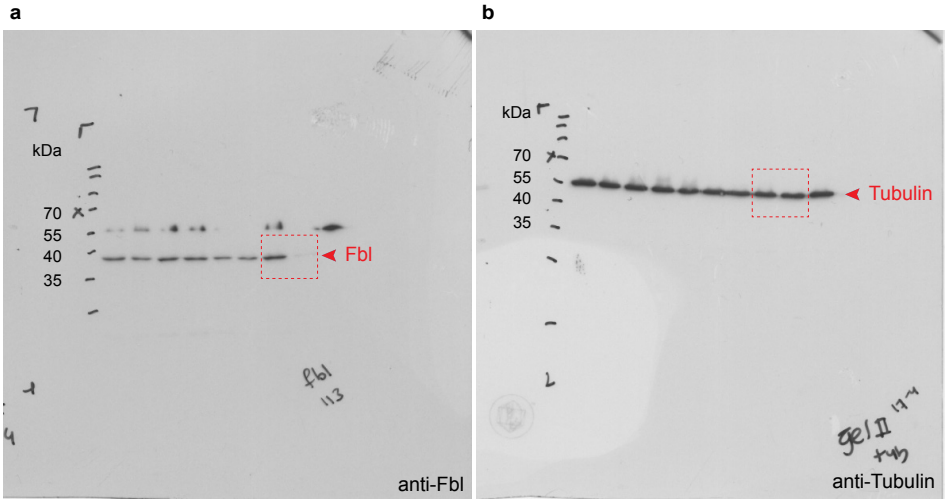

Original blots used for Figure 1h

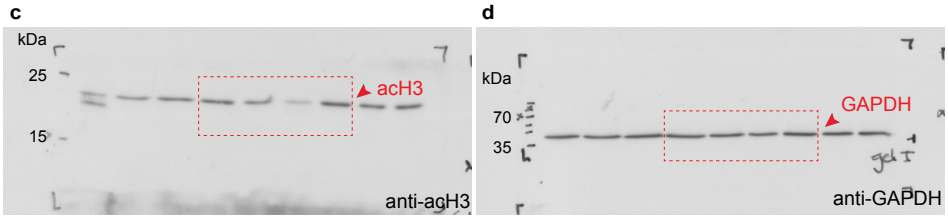

Original blots used for Supplementary Figure 8i

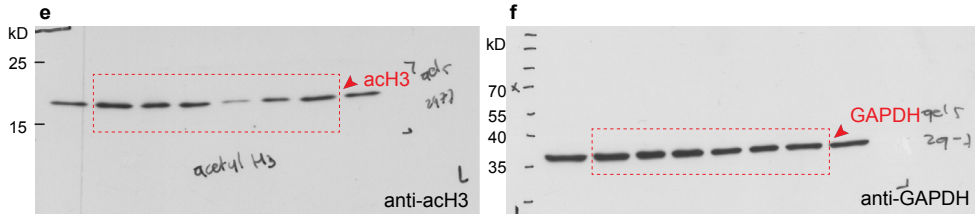

Supplementary Figure 15: Full uncut gel images for Western blots presented in Figures 1b and 1h and Supplementary Figure 8i. **a-b**. Full uncut gel images for the anti-dPANK/Fbl and anti-Tubulin Western blots presented in Figure **1b**. The part of the Western blot used for the figure is outlined by a dashed line. **c-d**. Full uncut gel images for the anti-acH3 and anti-GAPDH Western blots presented in Figure **1h**. The part of the Western blot used for the figure is outlined by a dashed line. **e-f.** Full uncut gel images for the anti-acH3 and anti-GAPDH Western blots presented in Supplementary Figure **8i**. The part of the Western blot used for the figure is outlined by a dashed line.

Original blots used for Supplementary Figure 12a (in the figure cut into two pieces)

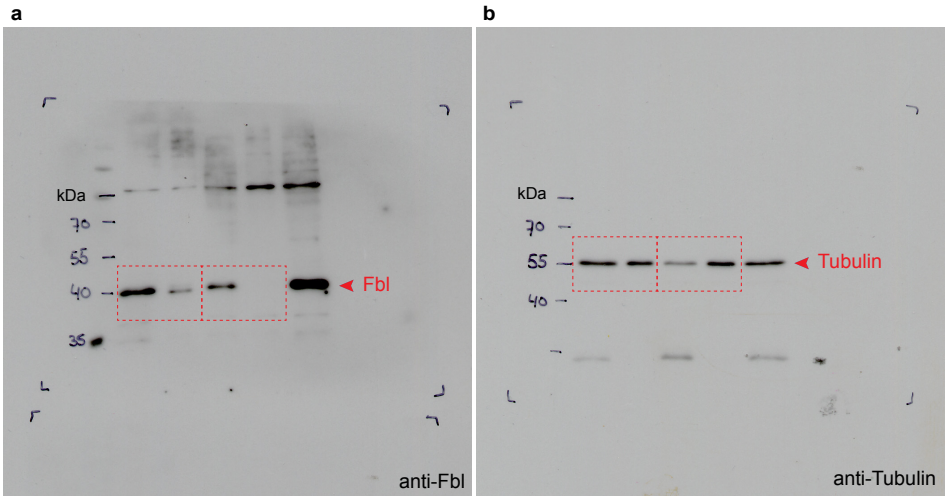

Original blots used for Supplementary Figure 14f

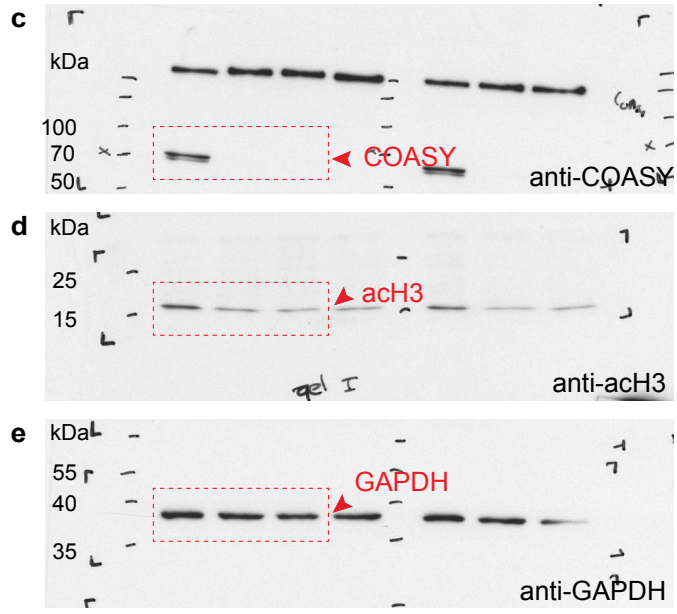

Supplementary Figure 16: Full uncut gel images for Western blots presented in Supplementary Figures 12a and 14f. a-b. Full uncut gel images for the anti-dPANK/Fbl and anti-Tubulin Western blots presented in Supplementary Figure **12a**. The part of the Western blot used for the figure is outlined by a dashed line. **c-e**. Full uncut gel images for the anti-COASY, anti-acH3 and anti-GAPDH Western blots presented in Supplementary Figure **14f**. The part of the Western blot used for the figure is outlined by a dashed line.

SUPPLEMENTARY NOTE

Synthesis of 4'-phosphopantetheine (PPanSH)

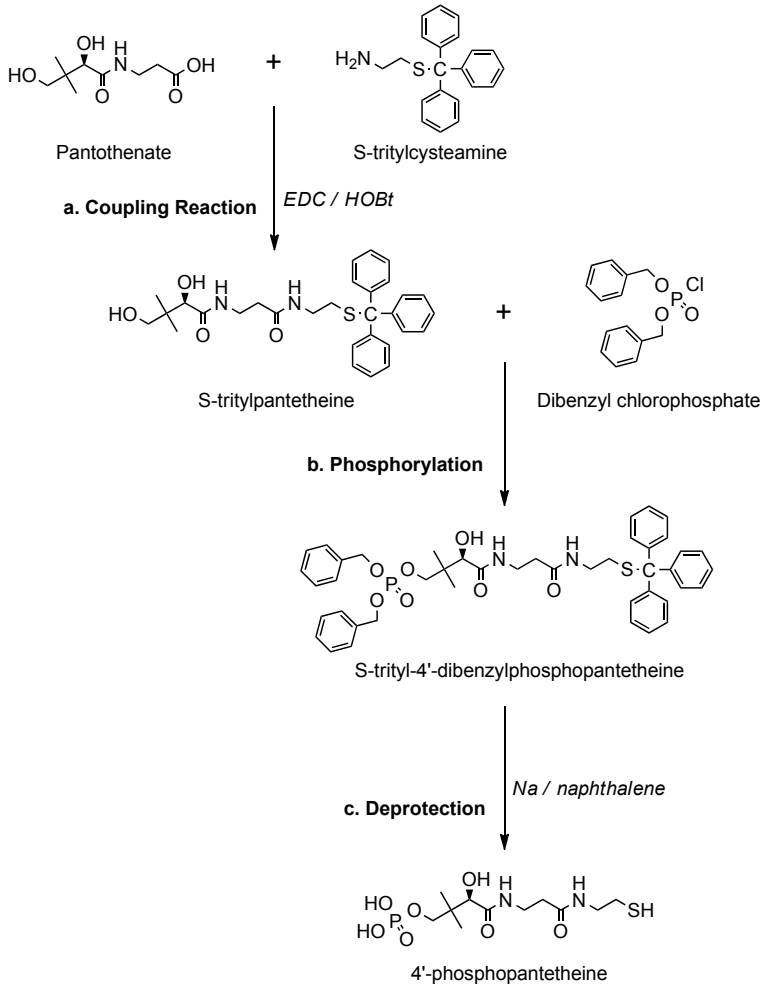

4'-Phosphopantetheine (PPanSH) Synthesis Protocol

4'-Phosphopantetheine (PPanSH) was synthesized in a three-step procedure as described below (a/b/c) (Supplementary Note). In the first step, commercially available pantothenic acid was coupled with synthesized S-tritylcysteamine. The obtained S-tritylpantetheine was then phosphorylated with freshly prepared dibenzylchlorophosphate. Finally, removal of benzyl groups provided 4'-phosphopantetheine.

D-Pantothenic acid was prepared from its hemicalcium salt (Aldrich, ≥ 99.0 %) by reacting with oxalic acid in distilled water. The precipitated calcium oxalate was filtered off, while the protonated form of D-pantothenic acid was obtained by evaporation of water. S-tritylcysteamine was synthesized from cysteamine hydrochloride and trityl chloride[1]. Dibenzylchlorophosphate was prepared by reacting dibenzylphosphite with N-chlorosuccinimide[2] in toluene as a solvent. All other chemicals were obtained from commercial sources and used without further purification; cysteamine hydrochloride (Aldrich, ≥ 98.0 %), trityl chloride (Aldrich, 97.0 %), N-(3-dimethylaminopropyl)-N'-ethylcarbodiimide (EDC) (Aldrich, ≥ 97.0 %), 1-hydroxybenzotriazole hydrate (HOBt) (Aldrich, ≥ 97.0 %), dibenzylphosphite (Aldrich, technical grade), N-chlorosuccinimide (Aldrich, 98 %). Column chromatography was carried out using Silica gel 60 Å, 60-100 mesh (Aldrich). Cation exchange chromatography was performed on DOWEX 50WX2, hydrogen form, 100-200 mesh (Aldrich). ^{1}H and ^{13}C NMR were recorded at 25°C with Varian Unity Inova 300 MHz spectrometer (300 MHz/75 MHz). The chemical shifts (δ) are reported in ppm units relative to TMS as an internal standard where spectra recorded in $CDCl_3$ or relative to residual solvent signal when D_2O was used. High-resolution mass spectra were obtained on AutospecQ mass spectrometer with negative electrospray ionization.

a) Coupling reaction – synthesis of S-tritylpantetheine

In dried acetonitrile (100ml) the following were prepared separately: (A) D-pantothenic acid (2.19g, 10.0mmol), (B) S-tritylcysteamine (3.19g, 10.0mmol) and (C) N-(3-dimethylaminopropyl)-N'-ethylcarbodiimide (EDC) (1.55g, 10.0mmol) together with 1-hydroxybenzotriazole hydrate (HOBt) (1.35g, 10.0mmol). After A, B and C were mixed together, triethylamine (10.4ml, 75mmol) was added. The mixture was stirred at room temperature for 24 h and quenched with addition of water (400ml). The product was extracted with diethyl ether (3x250ml). The combined organic phases were washed with 1 M hydrochloric acid, saturated aqueous solution of $NaHCO_3$ (500ml), and brine (500ml). The organic layer was dried over sodium sulfate and concentrated in vacuum S-tritylpantetheine (3.53g, 68%) was synthesized as pale-yellow crystals. ^{1}H NMR (300 MHz, $CDCl_3$) δ 0.85 (s, 3H), 0.92 (s, 3H), 2.29 (app t, J = 6.2 Hz, 2H), 2.38 (td, J = 2.3, 6.6, 6.8 Hz, 2H), 3.03 (m, 2H), 3.38-3.49 (m, 4H), 3.92 (s, 1H), 6.20 (t, J = 5.7 Hz, 1H, NH), 7.17-7.29 (m, 10 H), 7.36-7.45 (m, 5H).

b) Phosphorylation – synthesis of S-trityl-4'-dibenzylphosphopantetheine

Dibenzylchlorophosphate was freshly prepared by allowing a reaction of dibenzylphosphite (2.16g, 8.24mmol) with N-chlorosuccinimide (1.21g, 9.06mmol) in toluene (40ml) at room temperature for 2 h. The mixture was filtered and the filtrate was evaporated under vacuum and added to a solution of

S-tritylpantetheine (2.86g, 5.49mmol), diisopropylethylamine (3.06ml), 4-dimethylaminopyridine (0.067g, 0.55mmol) in dry acetonitrile (50ml). The mixture was stirred for 2 h at room temperature. Acetonitrile was removed under vacuum. Products were extracted into organic phase in dichloromethane (3x100ml) – aqueous $NaHCO_3$ (100ml) system. The organic extracts were washed with water (100ml), and dried over Na_2SO_4. Evaporation of solvent gave a crude S-trityl-4'-dibenzylphosphopantetheine as a dark brown oil (4.69g), which was further purified by flash chromatography (SiO_2, EtOAc, MeOH) to give a semicrystaline pale yellow product (0.640g, 0.82mmol). The yield of the synthesis and purification of S-trityl-4'-dibenzylphosphopantetheine is 15 %. ^{1}H NMR (300 MHz, $CDCl_3$) δ 0.75 (s, 3H), 1.03 (s, 3H), 2.32 (app t, J = 6.1 Hz, 2H), 2.4 (app t, J = 6.5 Hz, 2H), 3.06 (app q, J = 6.3 Hz, 2H), 3.47 (app q, 6.0 Hz, 2H), 3.60 (dd, J = 9.9, 7.3 Hz 1H), 3.85 (s, 1H), 4.00 (dd, J = 9.9, 7.0 Hz, 1H), 4.99-5.04 (m, 4H), 5.80 (t, J= 5.5 Hz, 1H, NH), 7.16-7.32 (m, 20H), 7.38-7.40 (m, 5H).

c) Deprotection – synthesis of 4'-phosphopantetheine

Naphthalene (12.9g, 100.6mmol) dissolved in tetrahydrofuran (70ml) was added to sodium metal (Na) (2.21g, 96.1mmol) in tetrahydrofuran (50mL). After 2 h the solution was cooled to –(35±5)°C and S-trityl-4'-dibenzylphosphopantetheine (1.85g, 2.37mmol) dissolved in tetrahydrofuran (70ml) was slowly added. The mixture was stirred for 2 h while maintaining the temperature below –30°C. The reaction was quenched by addition of water (100ml) and then dichloromethane (200ml) was added. Phases were separated and the aqueous phase (together 500ml) was washed with dichloromethane (200ml) and diethylether (3x200ml), concentrated under vacuum and passed through the cation exchange column (DOWEX 50WX2, 200g). Fractions were analyzed by LCMS and those containing the product were pooled and concentrated under vacuum. 4'-phosphopantetheine was precipitated with addition of $Ca(OH)_2$ as a calcium salt (332mg, 0.838mmol, 35%). The structure of the product was confirmed by comparison of NMR data with the literature[1,3] and by HRMS. ^{1}H NMR (300 MHz, D_2O) δ 0.86 (s, 3H), 1.08 (s, 3H), 2.54 (app t, J = 6.3 Hz, 2H), 2.87 (app t, J = 6.3 Hz, 2H), 3.43 (dd, J = 10.3, 5.0 Hz, 1H), 3.54 (m, 4H), 3.76 (dd, J = 10.3, 6.5 Hz, 1H), 4.14 (s, 1H). The HRMS mass for $C_{11}H_{22}N_2O_7SP$ $[M-H]^-$ was found to be 357.0880, which corresponds to the expected mass of 357.0885. The purity of the compound was determined to be >92%, using HPLC coupled with UV detection at 205nm.

SUPPLEMENTAL REFERENCES

1. Mandel, A.L., La Clair, J.J. & Burkart, M.D. Modular synthesis of pantetheine and phosphopantetheine. *Organic letters* **6**, 4801-4803 (2004).
2. Itoh, K., Huang, Z. & Liu, H.W. Synthesis and analysis of substrate analogues for UDP-galactopyranose mutase: implication for an oxocarbenium ion intermediate in the catalytic mechanism. *Organic letters* **9**, 879-882 (2007).
3. Lee, C.H. & Sarma, R.H. Inverstigation of the solution conformation of coenzyme A and its derivatives by hydrogen-1 and phosphorus-31 fast Fourier transform nuclear magnetic resonance spectroscopy. *Journal of the American Chemical Society* **97**, 1225-1236 (1975).